DESIGN AND CONSTRUCTION OF A FOLDING MECHANISM FOR A RADAR SYSTEM

A THESIS SUBMITTED TO
THE GRADUATE SCHOOL OF NATURAL AND APPLIED SCIENCES
OF
MIDDLE EAST TECHNICAL UNIVERSITY

BY

HÜNKAR KEMAL YURT

IN PARTIAL FULFILLMENT OF THE REQUIREMENTS
FOR
THE DEGREE OF MASTER OF SCIENCE
IN
MECHANICAL ENGINEERING

MAY 2019

Approval of the thesis:

DESIGN AND CONSTRUCTION OF A FOLDING MECHANISM FOR A RADAR SYSTEM

submitted by **HÜNKAR KEMAL YURT** in partial fulfillment of the requirements for the degree of **Master of Science in Mechanical Engineering Department, Middle East Technical University** by,

Prof. Dr. Halil Kalıpçılar
Dean, Graduate School of **Natural and Applied Sciences** _____

Prof. Dr. M. A. Sahir Arıkan
Head of Department, **Mechanical Engineering** _____

Assist. Prof. Dr. Ali Emre Turgut
Supervisor, **Mechanical Engineering, METU** _____

Prof. Dr. Eres Söylemez
Co-Supervisor, **Mechanical Engineering, METU** _____

Examining Committee Members:

Assoc. Prof. Dr. Mehmet Bülent Özer
Mechanical Engineering, METU _____

Assist. Prof. Dr. Ali Emre Turgut
Mechanical Engineering, METU _____

Prof. Dr. Eres Söylemez
Mechanical Engineering, METU _____

Assist. Prof. Dr. Ulaş Yaman
Mechanical Engineering, METU _____

Assist. Prof. Dr. Kutluk Bilge Arıkan
Mechanical Engineering, TEDU _____

Date: 14.05.2019

I hereby declare that all information in this document has been obtained and presented in accordance with academic rules and ethical conduct. I also declare that, as required by these rules and conduct, I have fully cited and referenced all material and results that are not original to this work.

Name, Surname: Hünkar Kemal Yurt

Signature:

ABSTRACT

DESIGN AND CONSTRUCTION OF A FOLDING MECHANISM FOR A RADAR SYSTEM

Yurt, Hünkar Kemal
Master of Science, Mechanical Engineering
Supervisor: Assist. Prof. Dr. Ali Emre Turgut
Co-Supervisor: Prof. Dr. Eres Söylemez

May 2019, 85 pages

In this thesis, a folding mechanism with 1 degrees of freedom is designed and constructed for a two-antenna radar system. The optimum mechanism for the problem is systematically selected among the conceptual mechanism alternatives. Then, a detailed synthesis and analysis study is performed on the selected mechanism, and the mechanism is implemented to the geometry of the radar system. By performing modal and strength analyses on the 3D model of the folding mechanism created during the implementation study, the design is improved and finalized according to the system requirements.

Keywords: Mechanism Synthesis, Folding Mechanism, Relative Motion Synthesis

ÖZ

RADAR SİSTEMİ İÇİN KATLANMA MEKANİZMASI GELİŞTİRİLMESİ

Yurt, Hünkar Kemal
Yüksek Lisans, Makina Mühendisliği
Tez Danışmanı: Dr. Öğr. Üyesi Ali Emre Turgut
Ortak Tez Danışmanı: Prof. Dr. Eres Söylemez

Mayıs 2019, 85 sayfa

Bu tezde, iki antenden oluşan radar sistemi için geliştirilen 1 serbestlik dereceli katlanma mekanizması sunulmuştur. Problem için gereksinimleri sağlayan uygun mekanizma çözümü, üzerinde kavramsal olarak çalışılan farklı mekanizma alternatifleri arasından sistematik olarak seçilmiştir. Seçilen mekanizma alternatifi üzerinde detaylı sentez ve analiz çalışmaları yapılmış ve mekanizma radar sistemine uyarlanmıştır. Geliştirilen katlanma mekanizmasının radar sistemine uyarlanması ile oluşturulan 3B model dosyası üzerinde modal ve statik mukavemet analizleri yapılarak, beklentiler doğrultusunda tasarım iyileştirilmiştir.

Anahtar Kelimeler: Mekanizma Sentezi, Katlanma Mekanizması, Bağıl Hareket Sentezi

To my lovely wife…

ACKNOWLEDGEMENTS

I would like to express my sincere gratitude to my co-supervisor Prof. Dr. Eres Söylemez for his encouragements, advice and insight throughout the research. I owe many thanks for his attitude which will guide me through the rest of my life.

I also would like to express my deepest gratitude to my supervisor Asst. Prof. Dr. Ali Emre Turgut for his guidance, endless support and helpful criticism throughout the progress of my thesis study.

I am severely grateful to the most beautiful part of my life, my wife Zeynep Öztürk Yurt. This thesis would not have been possible without the help, support and patience of her.

I am grateful to my family for their endless love and vulnerable support throughout my life.

I owe special thanks to my manager İsmail Güler and my colleagues Ekrem Fırtına and Sinan Yılmaz for their supports and presences in all phases of this study.

Finally, I am also grateful to ASELSAN Inc. that has given lots of opportunities to me to finish this study.

TABLE OF CONTENTS

LIST OF TABLES

TABLES

LIST OF FIGURES

FIGURES

LIST OF SYMBOLS

SYMBOLS

A#1	Antenna #1
A#2	Antenna #2
DoF	Degree of Freedom
F_{ij}	Force
M	Moment
θ_i	Joint variable of i^{th} link
a_i	Constant link length of i^{th} link
γ_i	Constant link angle of i^{th} link
CoG	Center of Gravity

CHAPTER 1

INTRODUCTION

1.1. Introduction to Early Warning Radar System

In today's world, Early Warning Radar (**Ra**dio **D**etecting **a**nd **R**anging) system is one of the significant defense systems which is developed to detect and track air breathing targets and missiles from very long ranges (~400 km). Also, the radar system is portable on tactical wheeled vehicles and transport aircrafts such as A400M and C130. Since the radar system is a highly mobile standalone system, it can be used at any where needed. [1]

The Early Warning Radar System consists of two antennas shown in Figure 1.1. The big antenna scans the environment by rotating, and it detects the targets from very long ranges. The other antenna called IFF (**I**dentification **F**riend or **F**oe) classifies the target as friend or foe.

Figure 1.1. Early Warning Radar System

1.2. Aim of the Study

The aim of the thesis is to develop a folding mechanism for the land platform - mobile air surveillance radar system that consists of two antennas that is conceptually given in Figure 1.1.

The main objective of the folding mechanism is to enable transition between the desired operating, maintenance and transport positions of the antenna pair. The antenna pair is mounted on the mechanical positioning unit (MPU) by means of the folding mechanism and the MPU rotates at 12 rpm with respect to the vehicle at the operating position.

Since the main objective of the radar system is to detect and track the targets from very long ranges, the folding mechanism should provide the required rigidity against external loads while conforming military standards in terms of accuracy, repeatability and strength.

1.3. Problem Definition

The section view of the folded antenna pair at the transport position can be seen in Figure 1.2. The big and small antennas are called as A#1 and A#2 respectively, and the physical properties of antennas are given in Table 1.1.

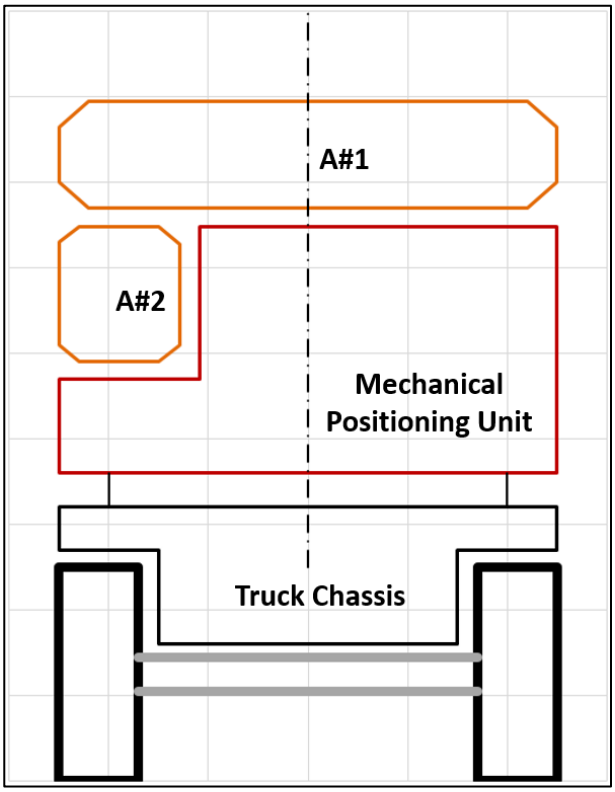

Figure 1.2. Section View of the Antenna Pair at the Transport Position

Table 1.1. *Physical Properties of Antennas*

	Mass [kg]	*Dimensions (Width, Height, Depth) [mm]*
A#1	5000	2500, 600, 5000
A#2	1000	600, 750, 3000

The desired positions of the antenna pair are given in Figure 1.3. In the transport position, which is given in Figure 1.3.a, the antenna pair folds into a volume such that the radar system can be carried by tactical wheeled vehicles and transport aircraft. During the operation, the antenna pair is positioned by an angle 75° with respect to

the ground, which is called as operating position and given in Figure 1.3.b. Desired duration of transition between operating and transport position is 1 minute.

Due to maintenance requirements of the radar system, the electronic units of antennas, which are placed behind, should be reachable. Therefore, in addition to the operating and transport positions, the maintenance position, where the antenna A#1 is perpendicular to the ground, should be provided by the folding mechanism. This position is given in Figure 1.3.c. However, there is no specified pose for the antenna A#2 in the maintenance position.

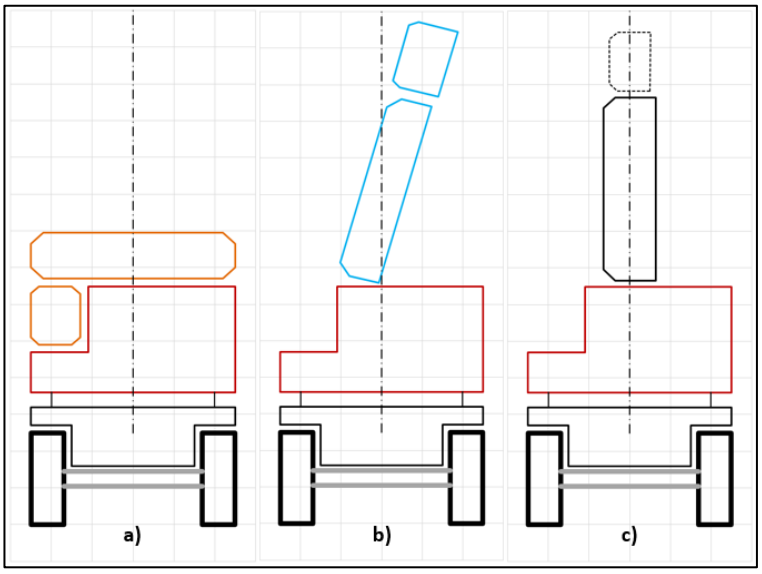

Figure 1.3. a) Transport position b) operating position c) maintenance position

As mentioned before, the rear side of the antenna A#1 is allocated for the electronic units. Therefore, the folding mechanism can hold the antenna chassis only from side walls. In other words, the folding mechanism cannot work behind the antenna.

Furthermore, the region that is located at the bottom of the A#1 is allocated for the components of the mechanical positioning unit, such as a motor, slip-ring, cooling units etc. For this reason, the antenna pair should not interfere with this region during the transition between the positions.

In case of power loss, the antenna pair must be able to fold into the transport position manually. Not only for the power loss case but also for reliability and repeatability of the system, the folding mechanism should have as few degrees of freedom as possible.

The radar system must be reliable under unexpected environmental conditions such as wind loads. According to requirements, the radar system must be able to withstand against winds up to 180 km/h, and should be able to unfold against to winds up 162 km/h.

1.4. Literature Survey

Since the radar system is a military product, resources about equivalent systems are quite limited in literature. Therefore, only accessible information documents are investigated for the equivalent foldable radar systems.

First one of the equivalent products is ISKRA® 80K6(M) Air Surveillance Radar System from Ukraine [2]. Folded and unfolded positions of the antenna pair are given in Figure 1.4 and Figure 1.5 respectively.

Figure 1.4. Folded Position of ISKRA® - 80K6(M) [2]

Figure 1.5. Unfolded Position of ISKRA® - 80K6(M) [2]

The kinematic chain of the folding mechanism consists of a combination of inverted slider crank and four bar mechanisms with 4 DOF. The kinematic chain is given in Figure 1.6. The mechanism is placed at the back side of the antenna on the two different parallel planes. In the application, 6 actuators are used to drive the mechanism.

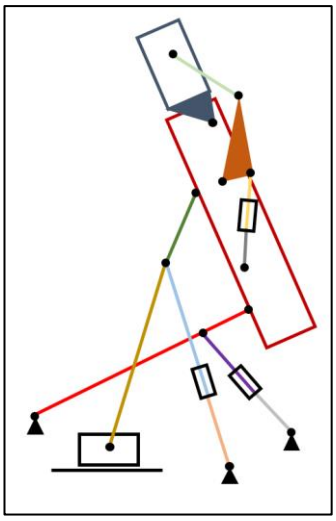

Figure 1.6. The kinematic chain of ISKRA® - 80K6(M)

Another example is Ground Master 400 by Thales® and Raytheon® from US [3], shown in Figure 1.7 and Figure 1.8.

Figure 1.7. Unfolded Position of Ground Master 400 [3]

Figure 1.8. Folded Position of Ground Master 400 [3]

The kinematic chain of the mechanism with 2 DOF is given in Figure 1.9. The bigger antenna is mounted on the chassis by means of a four-bar mechanism, and it is driven by an actuator, which is placed in the configuration of inverted slider crank. The IFF antenna is mounted on the bigger antenna with a hinge and it can be rotated independently.

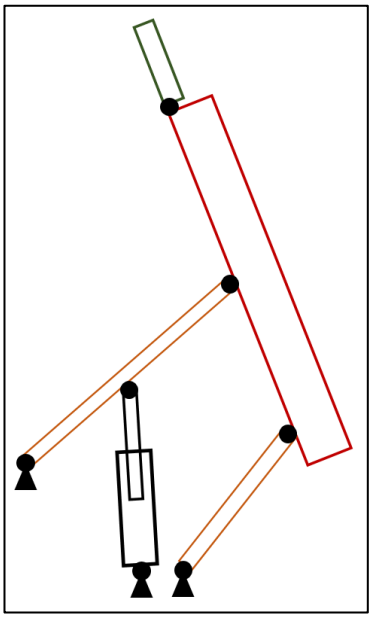

Figure 1.9. The Kinematic Chain of Ground Master 400

The last equivalent product which is given in Figure 1.10 is AN/TPS – 75 by Raytheon® [4].

Figure 1.10. Unfolded Position of Raytheon® AN/TPS – 75 [4]

The kinematic chain of the mechanism is given in Figure 1.11. A slider-crank mechanism is synthesized to mount and rotate the bottom antenna. On the other hand,

the top antenna is mounted with a hinge to the bottom antenna and actuated by means of a four-bar mechanism which is in the configuration of lifting jack. Conceptually, the mechanism has 2 DOF. However, by means of a driveline design, 2 DOFs are dependent to each other. Therefore, the actual DOF of the mechanism reduces to 1.

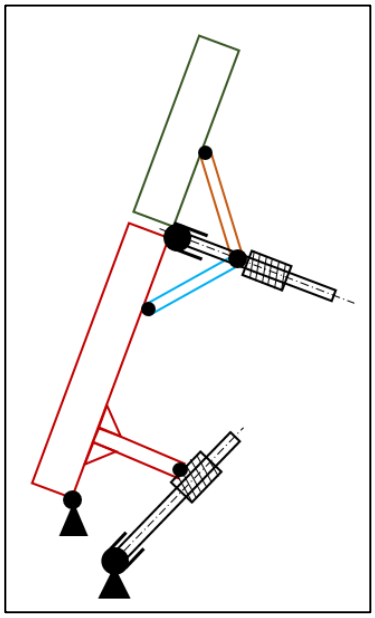

Figure 1.11. The Kinematic Chain of Raytheon® AN/TPS - 75

As mentioned before, resources such as patents and papers about equivalent radar systems are quite limited in the literature. Therefore, folding mechanisms of hardtop convertible vehicles which are based on a similar principle are investigated as well. The reason is that almost all of hardtop convertible vehicles consist of front and rear roof parts, and most of the mechanisms used to fold the roof pair have 1 DOF. [5]

The folding mechanism, which is the closest application to our problem is patented by Queveau G.P. and Guillez J.M. in 2002 [6]. In this application, the front and rear roof parts form two links of a four-bar mechanism. In addition to the roof part pair, the central roof part is also placed by a four-bar mechanism. However, thanks to relative motion synthesis, the second four-bar mechanism is driven by the input link of the first four-bar mechanism simultaneously. Thus, three roof parts can be moved

synchronously by a folding mechanism which has only 1 DOF. A drawing from the patent is given in Figure 1.12.

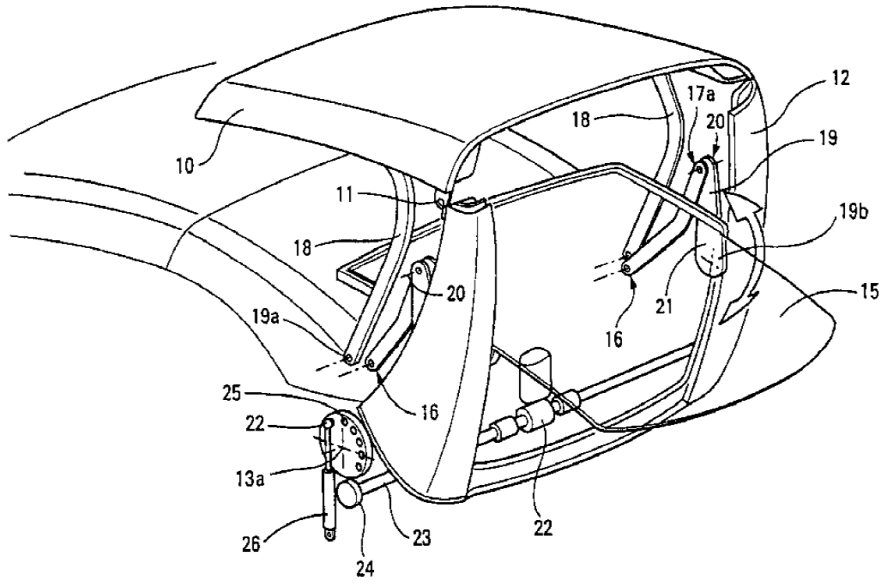

Figure 1.12. The Folding Mechanism of a Hardtop Convertible Vehicle [6]

1.5. Thesis Outline

In this thesis, the development of a folding mechanism for a radar system is presented. The details of the design process are indicated in the following chapters.

In Chapter 2, conceptual design of the mechanism is presented. As the first step, the mechanism alternatives are created conceptually. Then concept evaluation variants are defined, and alternatives are evaluated according to the design criteria by the experienced design engineers. Thus, the best mechanism is selected systematically among the alternatives.

In Chapter 3, detailed synthesis and analysis studies on the selected mechanism are described. The synthesis study is performed for desired positions of the antenna pair with respect to the geometric restrictions. Then, a kinematic analysis is performed to

analyze the motion of the mechanism. In addition to the kinematic analysis, a force analysis is also performed to determine the joint forces during the motion.

In Chapter 4, the implementation of the design is given. The links of the mechanism are sized with respect to the exposed joint forces. Then, a modal and strength analyses are performed on the design of the folding mechanism by using the finite element method. According to the simulation results, the mechanism is improved.

In Chapter 5, the results of the study are discussed. Also, some recommendations are given for future work and further improvements on the study.

CHAPTER 2

CONCEPTUAL DESIGN

2.1. Introduction

In the conceptual design stage, the main objective is to develop different mechanism alternatives and then choose the best solution for the problem among the alternatives. Since the radar system consists of two antennas, the required folding mechanism is separated into two different sections for A#1 and A#2. Since A#1 is bigger and heavier than A#2, the mechanism for A#1 is studied at first, then the mechanism for A#2 is developed on it dependently.

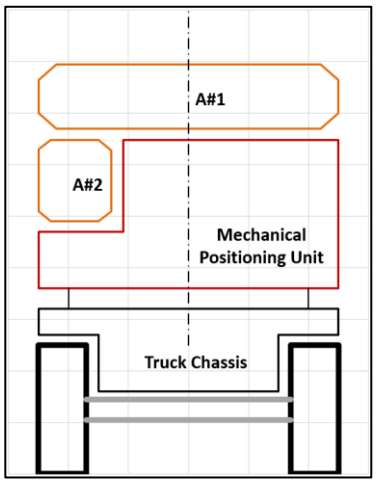

Figure 2.1. Section View of the Antenna Pair at the Transport Position

In order to select the best solution among alternatives, the simpler version of the conceptual design procedure, which is defined by Pahl and Beitz, is used by defining concept evaluation criteria [7]. To perform the evaluation study as objective as possible, a group of engineers who work on the same project participated in the evaluation study.

2.2. Concept Development for A#1

In the light of the literature survey, four different mechanism alternatives are created for the A#1. The primary expectation is to provide the required operating, maintenance and transport positions for A#1 kinematically.

According to the given requirements, the direction of the signal receiving surface of A#1 is not restricted in the transport position. In other words, it can be placed both facing upwards or downwards as shown in Figure 2.2. If the antenna is placed upwardly directed, the developed mechanism must rotate the antenna 75°. Otherwise, the antenna must be rotated by an angle of 105° between the desired transport and operating positions. Since the antenna should be rotated 105° with respect to the ground, the antenna can be held at 90° positioned between the operating and transport positions for maintenance purposes.

On the other hand, the downwardly directed antenna has a crucial advantage since it is protected against physical effects during transportation, and the backside of the antenna is reachable at transport position as well.

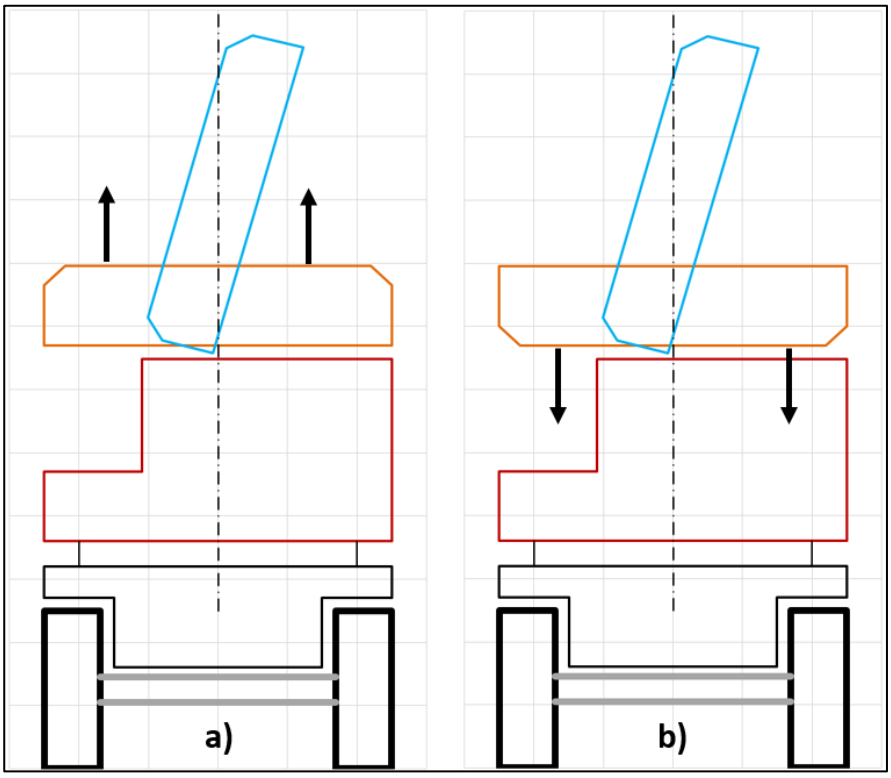

Figure 2.2. a) Upwardly Directed b) Downwardly Directed

2.2.1. Concept #1

The first mechanism alternative for A#1 is inverted slider-crank mechanism with 1 DoF, which can be seen in almost all dump trucks. The sliding joint of the slider-crank mechanism is in the form of piston-cylinder arrangement. In this alternative, the antenna A#1 should to be placed upwardly directed in the transport position, and it is rotated by an angle of 75°. An illustrative sketch of Concept #1 is given in Figure 2.3.

Since the antenna should not interfere with the allocated region, the pivot for desired positions is calculated as shown with a black circle in Figure 2.3. Therefore, the geometric center of A#1 is positioned almost 500 mm away from the center axis in the operating position. For this reason, the rotation axis cannot overlap with the symmetry axis of the radar system. Additionally, the actuators must be extended further for the maintenance position.

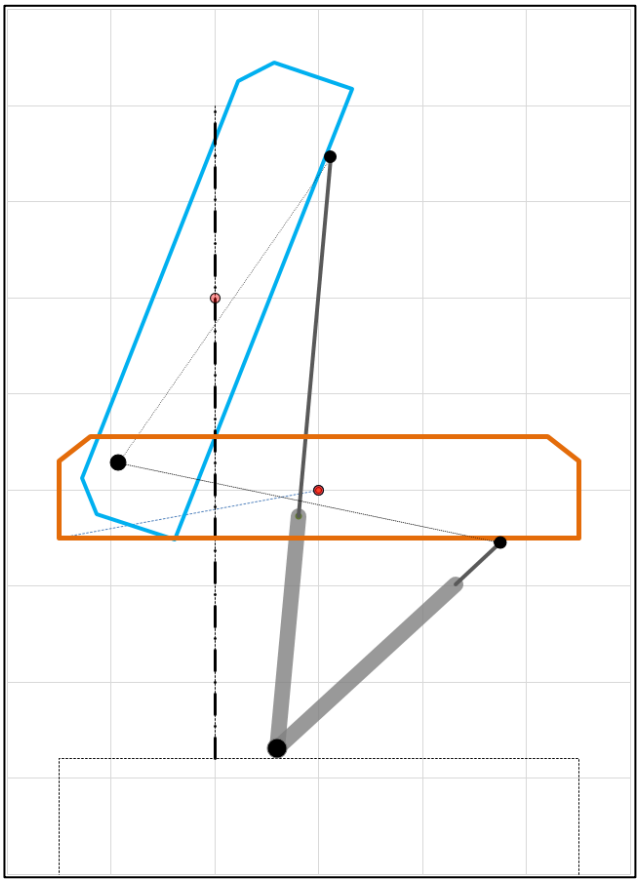

Figure 2.3. An Illustrative Sketch of Concept #1

2.2.2. Concept #2

The second mechanism alternative is a planar five-link mechanism with 2 DOFs which is also known as a planar parallel manipulator in literature. Since the mechanism has 2 DOFs, this alternative enables the antenna to translate in the horizontal axis while maintaining the angle of A#1 about the normal axis. This capability can be used to balance the antenna system about the rotation axis at different antenna angles when needed. A descriptive sketch of Concept #2 at desired positions is given in Figure 2.4.

In this alternative, the antenna A#1 can be directed upwardly or downwardly in the transport position. In Figure 2.4, A#1 is placed downwardly directed.

Additionally, since the planar mechanism has 2 DOF, the actuators must be driven synchronously based on the inverse kinematic analysis of the mechanism.

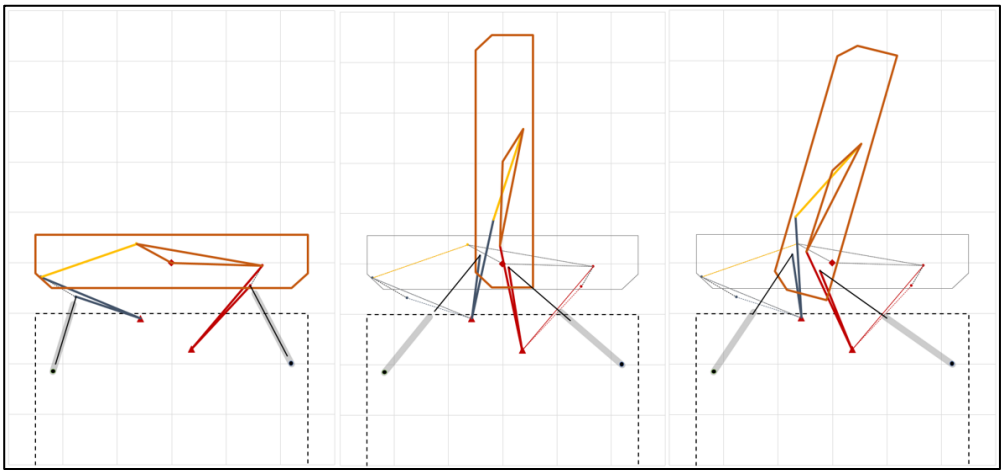

Figure 2.4. A Descriptive Sketch of Concept #2 at Desired Positions

2.2.3. Concept #3

The third concept is developed by using a four-bar mechanism. The antenna A#1is the coupler link of the four-bar mechanism. Also, the antenna A#1 can be placed downwardly directed as in the previous concept.

An explanatory sketch of the mechanism at desired positions is given in Figure 2.5. The crank link of the mechanism is driven by an actuator that can be placed in inverted slider crank configuration.

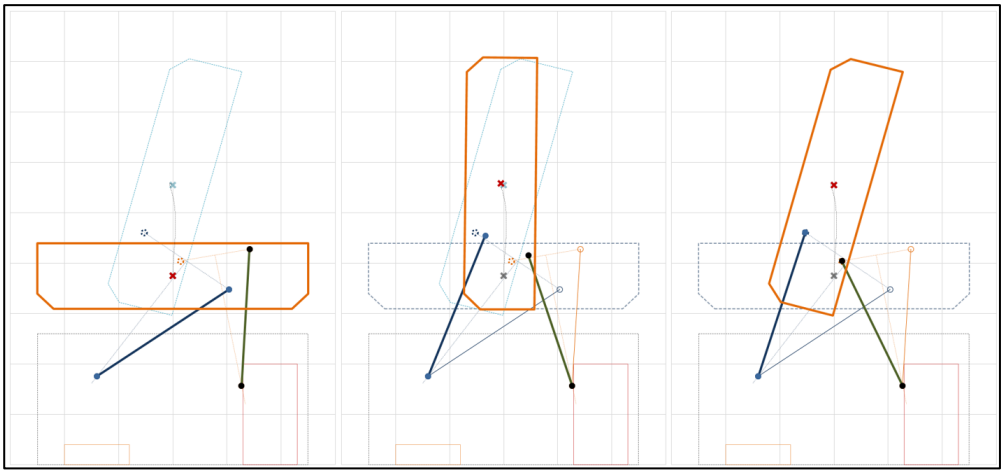

Figure 2.5. An Explanatory Sketch of Concept #3 at Desired Positions

2.2.4. Concept #4

The last concept comprises a slider crank mechanism. As in the previous concept, the antenna is placed downwardly directed, and it forms the coupler link of the mechanism. In addition to driving the mechanism, the slider of the mechanism takes on the task of mounting the antenna to the chassis.

A descriptive sketch of the mechanism at desired antenna positions is given in Figure 2.6.

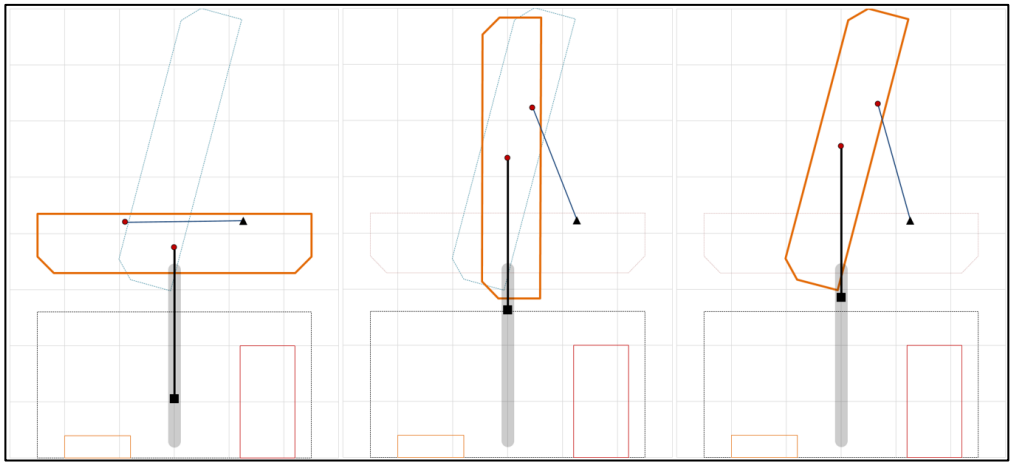

Figure 2.6. A Descriptive Sketch of Concept #4 at Desired Positions

2.3. Concept Evaluation Criteria for A#1

In order to perform the evaluation of concepts procedure on the alternatives for A#1, the evaluation criteria for the problem should be clearly defined such that concepts should be comparable to each other. These evaluation criteria can be selected among the technical issues such that the mechanism will comply with the rigidity, reliability, producibility, repeatability and mountability requirements which are significant for military systems.

The following criteria are chosen for the evaluation of concepts.

- High rigidity: Since the accuracy and repeatability are quite important for the radar system, the antenna pair must be held as rigid as possible against exposed external loads.
- Small number of links: The number of links influences design, production and assembly stages of the project directly. In addition, having a small number of links is also important for the accuracy of the mechanism.
- Simple actuator requirement: Minimum force and stroke requirement of the mechanism provides a significant advantage in terms of using off the shelf actuators. In addition, a simple kinematic relation between the actuator stroke and the antenna angle is an advantage to use a simple driver algorithm.
- Ease of assembling: Since the antenna pair is quite heavy and big, the ease of integration of the mechanism is critical for the assembly stage.
- Direct measurement of antenna angle: Since the antenna tracks targets from very long ranges, the measurement of the antenna angle is significant in terms accuracy. Therefore, direct measurability of the antenna angle is a huge advantage.
- Pose of antenna: The poses of A#1 at transport and operating positions are crucial for the system.
- Ease of actuation of A#2: If the mechanism offers an opportunity to drive A#2 by the same actuation simultaneously, A#2 can be driven without an additional actuator.

2.4. Evaluation of Concepts for A#1

With the availability of evaluation criteria, the concepts can be evaluated subjectively to choose the best alternative for the problem. Since the evaluation is a subjective procedure, the experiences of the designer are quite important for this stage.

As a first step, the weight factors of each criterion are calculated. To do this, weights are defined from zero to ten with respect to its importance for the problem. Then, a

weight factor for each criterion is calculated by dividing the weights to the sum of the defined all weights. In Table 2.1, weights and calculated weight factors are shown.

Table 2.1. *Weight Factors of Evaluation Criteria*

Evaluation Criteria	*Weight (0 – 10)*	*Weight Factor*
High Rigidity	9	0.170
Small Numbers of Links	7	0132
Simple Actuator Requirement	8	0.151
Easy Assembling	6	0.113
Direct Measurement of Antenna Angle	7	0.132
Pose of Antenna	9	0.170
Easy Actuation of A#2	7	0.131
TOTAL	53	1

In order to evaluate concepts systematically, the values which are given with their meanings in Table 2.2 will be assigned to each concept.

Table 2.2. *The Value Scale for the Evaluation of Concepts*

Points	*Meaning*
0	Absolutely useless solution
1	Very inadequate solution
2	Weak solution
3	Tolerable solution
4	Adequate solution
5	Satisfactory solution
6	Good solution with few drawbacks
7	Good solution
8	Very good solution
9	Solution exceeded the requirement
10	Ideal solution

As a final step, the concepts are evaluated by assigning values subjectively with respect to the defined criteria. As seen in Table 2.3, Concept #4 (Figure 2.6), which comprises a slider crank mechanism, is selected to be the best concept among alternatives for the antenna A#1.

Table 2.3. *Weight Factors of Evaluation Criteria*

Evaluation Criteria	*Weight Factor*	*Concept #1*	*Concept #2*	*Concept #3*	*Concept #4*
High Rigidity	0.170	9	5	7	8
Small Numbers of Links	0132	9	5	6	8
Simple Actuator Requirement	0.151	6	6	6	8
Easy Assembling	0.113	8	5	6	7
Direct Measurement of Angle	0.132	9	6	6	8
Pose of Antenna	0.170	2	8	8	8
Easy Actuation of A#2	0.131	6	5	8	7
TOTAL	1	6.849	5.792	6.774	7.755

2.5. Concept Development for A#2

After the mechanism concept for the A#1 is chosen, the next step is to develop a mechanism for A#2 which can be driven by the first mechanism at the same time.

The desired poses for A#2 at operating and transport positions are given in Figure 6. As mentioned before, there is no specified pose for A#2 at the maintenance position. When the desired positions of A#2 are investigated, it can be easily seen that A#2 should be rotated 195° with respect to the ground. However, A#2 rotates only 90° relative to A#1 between desired positions.

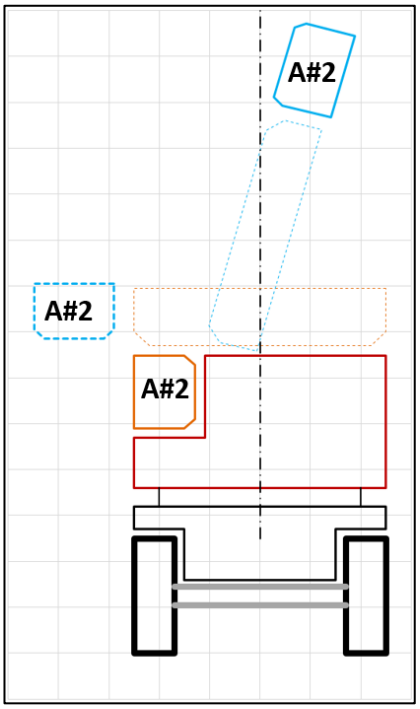

Figure 2.7. Desired Poses of A#2

Since the mechanism is expected to rotate A#2 only 90° on A#1, a four-bar mechanism concept is preferred for A#2. Nevertheless, the four-bar mechanism can be synthesized in several different configurations. For that reason, two different concepts are created and evaluated for A#2.

2.5.1. Concept #1

In the first concept, the antenna A#2 forms the coupler link of the four-bar mechanism which mounts the A#2 to the A#1 at the same time. In Figure 2.8, an illustrative sketch of the mechanism is given.

Since the antenna acts as the coupler link of the four-bar mechanism, it can be held rigidly by the other two links of the mechanism from two distinct points. Additionally, one of the links, which are hinged to A#1 and indicated by green and red in Figure 2.8, can be selected freely as the crank, and it can be driven by the other mechanism developed for A#1.

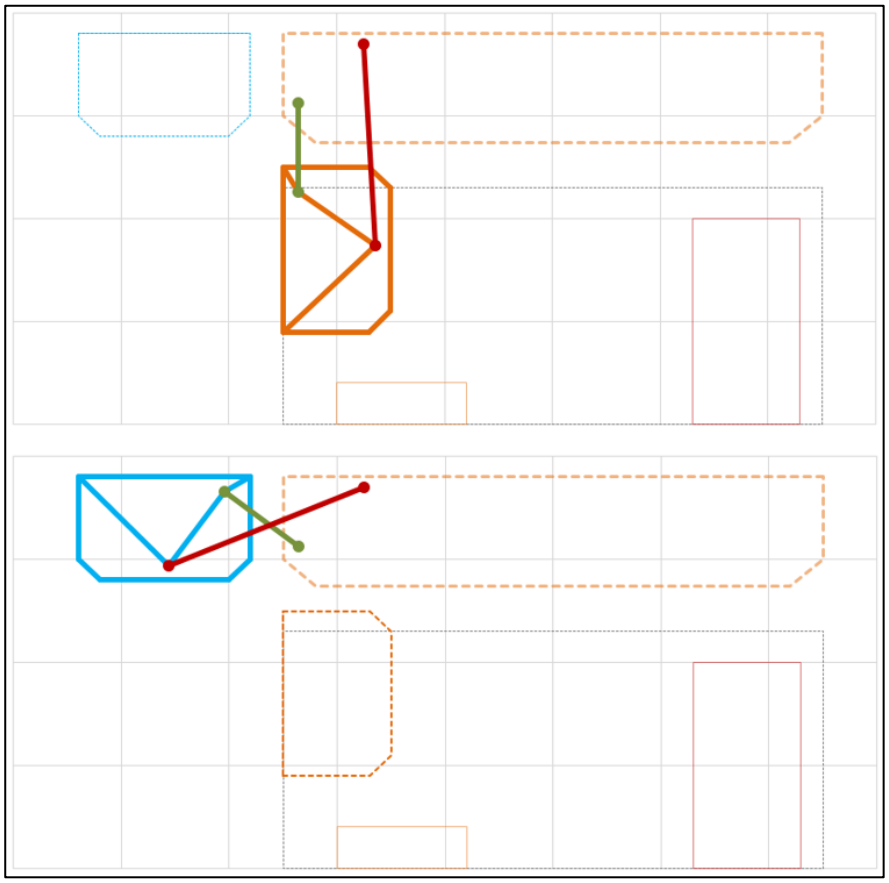

Figure 2.8. An Illustrative Sketch of Concept #1

2.5.2. Concept #2

In the second concept, A#2 is rotated about the pivot which is calculated for desired positions. In other words, A#2 is simply hinged on A#1. A descriptive sketch of the concept is shown in Figure 2.9.

In addition to the simple structure, the link which connects A#2 to A#1 can be driven easily by the other mechanism.

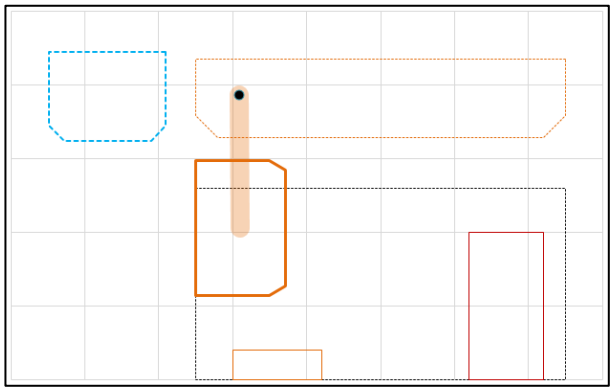

Figure 2.9. A Descriptive Sketch of Concept #2

2.6. Concept Evaluation Criteria for A#2

As done before, the evaluation of concepts procedure is performed on the folding mechanism concepts of A#2 to choose the best solution.

Similar to the previous procedure, the following criteria with the same explanations, which are defined for the mechanism of A#1, are selected for the evaluation of concepts:

- High rigidity
- Small number of links
- Easy assembling

2.7. Evaluation of Concepts for A#2

Firstly, weights are assigned to criteria and weight factors are calculated for each criterion. The tabulated weights and weight factors are given in Table 2.4.

Table 2.4. *Weight Factors of Evaluation Criteria*

Evaluation Criteria	*Weight (0 – 10)*	*Weight Factor*
High Rigidity	9	0.391
Small Numbers of Links	7	0.304
Easy Assembling	7	0.304
TOTAL	23	1

After weight factors are obtained, the next step is the evaluation of concepts. To do this, the values, which are given with their meanings in Table 2.2, are assigned to the criteria for each concept as done before.

The result of the evaluation is given in Table 2.5. As seen in the table, Concept #2 is evaluated as the best solution for A#2.

Table 2.5. *Evaluation of Concepts*

Evaluation Criteria	*Weight Factor*	*Concept #1*	*Concept #2*
High Rigidity	0.391	8	7
Small Numbers of Links	0.304	6	8
Easy Assembling	0.304	6	8
TOTAL	1	6.783	7.609

2.8. The Final Mechanism Concept for the Antenna Pair

Based on the evaluation studies, the final mechanism concept for the antenna pair is formed, given in Figure 2.10. During the detailed design stage, the selected mechanisms for each antenna will be synthesized according to the desired antenna positions, and they will be connected to each other by means of an additional mechanism which will provide the required relative motion of A#2 with respect to A#1.

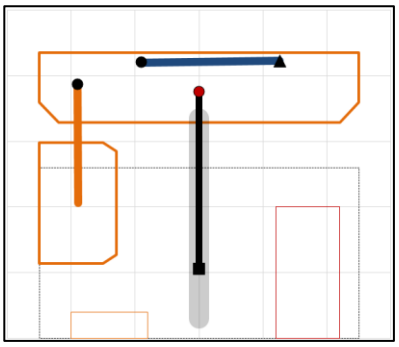

Figure 2.10. The Final Mechanism Concept for the Antenna Pair

CHAPTER 3

DETAILED SYNTHESIS AND ANALYSIS OF THE MECHANISM

3.1. Introduction

In the detail design stage, the selected mechanism concepts for A#1 and A#2 are synthesized in detail by considering geometric restrictions. Then, in order to obtain the required relative motion between antennas, the synthesized mechanisms are connected to each other by means of an additional mechanism.

After synthesis studies are finalized, the resultant mechanism is kinematically analyzed to check motion requirements and geometric restrictions. In addition to the kinematic analysis, a force analysis is performed for the resultant mechanism to size links, components, such as bearings, sliders, and actuators etc., with respect to the exposed force and torque loads. Therefore, this stage is not only the most important but also the most time – consuming part of the study.

3.2. Kinematic Synthesis of the Mechanism for A#1

As the first step of the kinematic study, a slider – crank mechanism is synthesized for the desired positions of A#1 by considering geometric constrains. In literature, the problem is known as analytical synthesis of four bar linkage for prescribed positions. With the synthesis study, all constant parameters of the mechanism are derived parametrically.

At the beginning of the synthesis study, the desired motion of the antenna and geometric constraints are defined clearly. Then, the slider – crank mechanism is synthesized analytically according to the specified parameters.

3.2.1. Geometric Constraints for A#1

Some geometric constraints are defined according to the required performance expectations and some regulations that the radar system must comply with. The geometric constraints are shown in Figure 3.1.

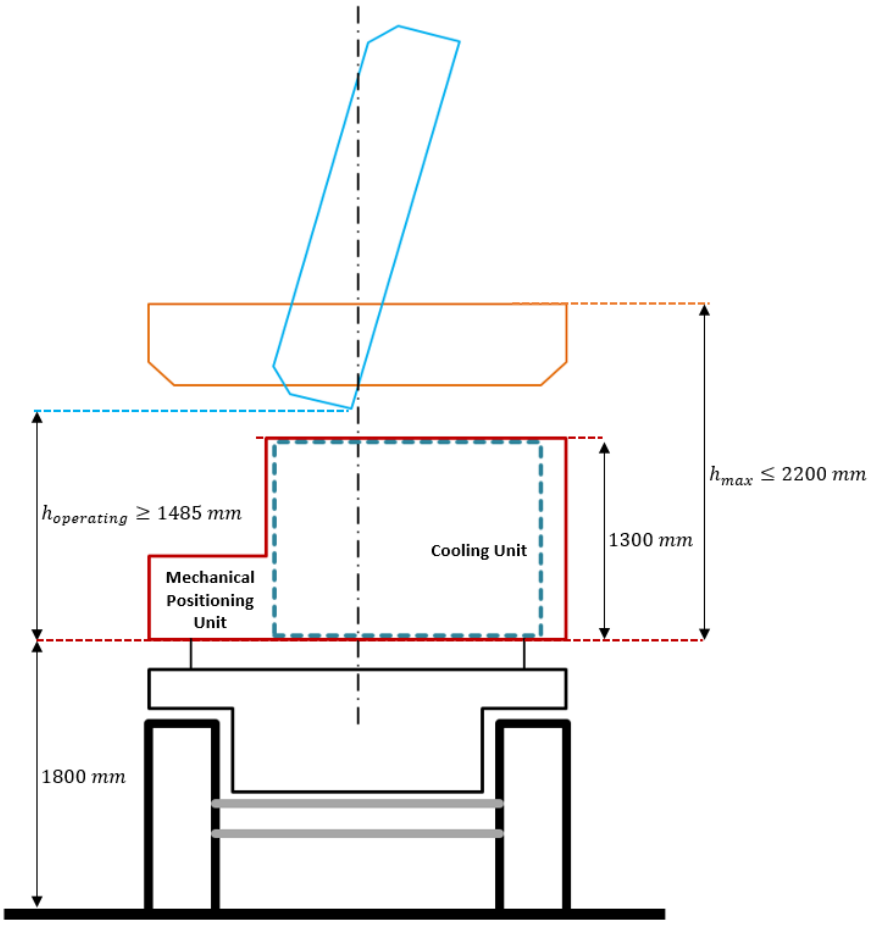

Figure 3.1. Geometric Constraints for A#1

Since the radar system is portable on tactical wheeled vehicles and transport aircrafts, the sizes of the radar system in transport position must comply with the related regulations. According to the road traffic regulations in Turkey, the maximum permitted height for vehicles is 4 meters. Therefore, the rear side of A#1 in transport

position must be positioned at most 2200 mm above the bottom level of mechanical positioning unit.

The second constraint is that the bottom corner of A#1 must be at least 1485 mm above the bottom level of mechanical positioning unit. With this restriction, the antenna is able to scan the environment without being shadowed by the vehicle.

In addition to the defined restrictions, as mentioned before, there is an allocated region for some components that antenna pair should not interfere while moving. The size of the cooling unit specifies the minimum height of the region. For this reason, the minimum height of the swept volume during the movement of A#1 should be 1300 mm above the bottom level of the mechanical positioning unit.

Lastly, since the radar system is quite heavy and wide, the main bearing location on A#1 is also crucial for the chassis of A#1 because of the exposed loads. Therefore, the main bearing location C is determined at the beginning of the study. Thus, the chassis will be designed with the required rigidity and strength for the decided bearing location that is given in Figure 3.2. Furthermore, the bearing location is also significant for the balancing studies that may be needed in the future.

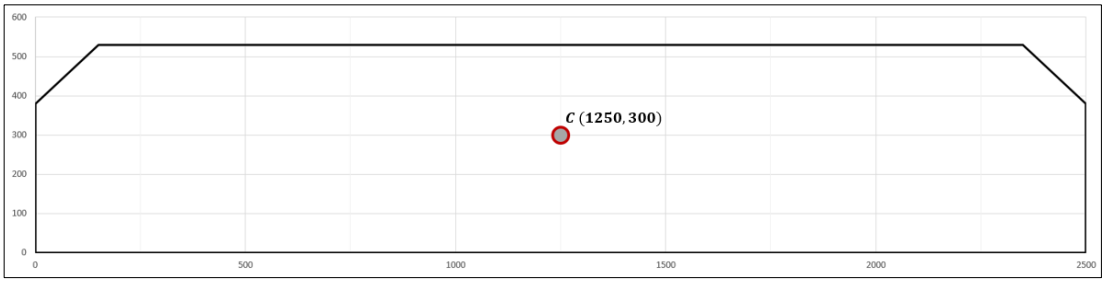

Figure 3.2. Selected Bearing Location on A#1

3.2.2. Desired Positions of A#1

As specified before, the synthesis study is performed for the desired motion of the prescribed positions of A#1. And, the positions are defined with respect to the selected

bearing location C by considering the geometric restrictions. In addition, the intersection point of the center axis and the bottom level of the mechanical positioning unit is assumed to be the origin for further studies.

The first position represents the transport position of A#1 that can be seen in Figure 3.3, and the point C located on {0,1875} position by an angle 180° such that the rear side of the antenna is 2175 mm above.

The second position is arbitrarily selected between the transport and operating position at this stage. However, this freedom will provide a remarkable opportunity to optimize the swept volume in the future. The selected second position of A#1 is given with a dashed line in Figure 3.3.

The third position is defined for the operating position of A#1 such that the bearing location C is located on {0, 2775} by the desired antenna angle 75° with respect to the ground. At this position, the bottom corner of A#1 is almost 1490 mm above. Indeed, the location of point C is calculated according to this geometric restriction by keeping the potential energy change as minimum as possible. The third position is shown in Figure 3.3.

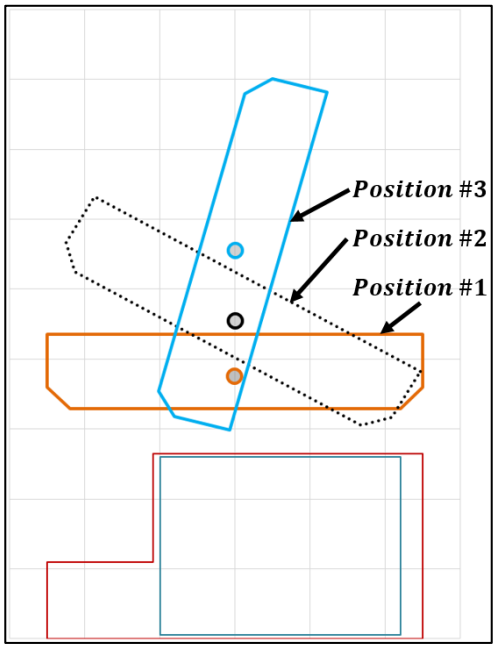

Figure 3.3. Three Prescribed Positions of A#1

3.2.3. Synthesis of the Slider – Crank Mechanism

As specified in the previous section, the main bearing location on A#1, that is called as the point C, is selected with the design engineer of A#1. Additionally, according to the desired positions of the point C, the direction of sliding is also formed dependently. Therefore, the crank link of the mechanism is the only unknown of the problem.

In order to synthesize the slider – crank mechanism analytically, the crank link of the mechanism is represented in dyad form for desired antenna positions, and the loop – closure equations are written for the vector pairs to obtain center and circle point curves. After the center and circle points are obtained, the solution family for the crank link can be investigated on the system. Then, the resultant crank link is synthesized for the selected fixed pivot which is defined with respect to the obtained center points [8][9].

By considering the prescribed positions, the crank link is represented in dyad form, which is given in Figure 3.4.

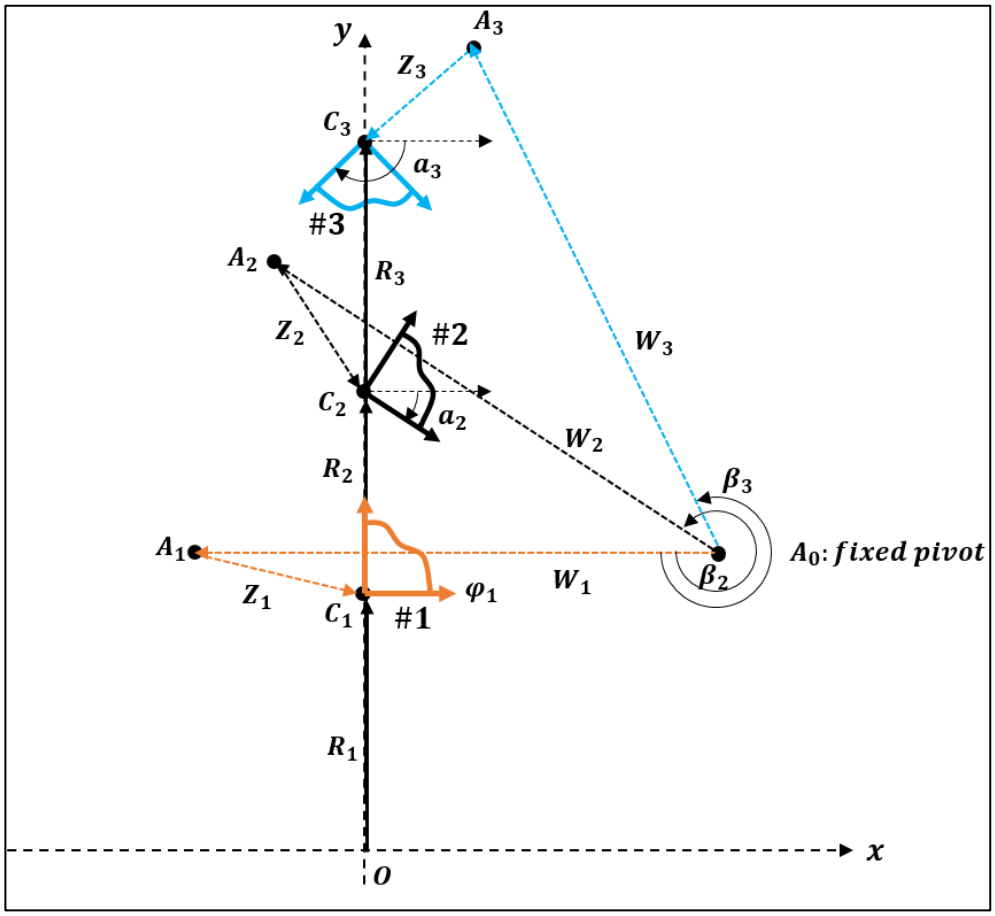

Figure 3.4. The Dyad Representation of the Crank Link

For the three prescribed positions, the vectors $\vec{R}_i$ and the angle values φ_i are written as below. $\left(\vec{R}_i, \varphi_i; i = 1,2,3\right)$

$$\vec{R}_1 = 0 + 1875i \tag{3.1}$$

$$\vec{R}_2 = 0 + 2275i \tag{3.2}$$

$$\vec{R}_3 = 0 + 2775i \tag{3.3}$$

$$\varphi_1 = 0° \tag{3.4}$$

$$\varphi_2 = -30° \tag{3.5}$$

$$\varphi_3 = -105° \tag{3.6}$$

Note that, the vector $\vec{R}_2$ and the angle value φ_2 are arbitrarily selected as specified before.

3.2.3.1. Circle and Center Points of the Crank Link

According to the values, the relative displacement vectors $\vec{\delta}_j$ and angles α_j are calculated as well. $\left(\vec{\delta}_j, \alpha_j ; j = 1,2\right)$

$$\vec{\delta}_1 = \vec{R}_2 - \vec{R}_1 \tag{3.7}$$

$$\vec{\delta}_2 = \vec{R}_3 - \vec{R}_1 \tag{3.8}$$

$$\alpha_1 = \varphi_2 - \varphi_1 \tag{3.9}$$

$$\alpha_2 = \varphi_3 - \varphi_1 \tag{3.10}$$

The equation set for the dyad representation of the crank link is written as below.

$$\vec{\delta}_1 = \vec{W}\left(e^{i\beta_1} - 1\right) + \vec{Z}\left(e^{i\alpha_1} - 1\right) \tag{3.11}$$

$$\vec{\delta}_2 = \vec{W}\left(e^{i\beta_2} - 1\right) + \vec{Z}\left(e^{i\alpha_2} - 1\right) \tag{3.12}$$

To solve the equation set for $\vec{W}$ and $\vec{Z}$, the free parameters β_1 and β_2 must be assumed. The variable β_2 defines the total rotation of the crank link during the transition between the operating and transport positions. Therefore, the free parameter β_3 can be selected intuitively by imagining the motion of the crank link during the transition. For the solution, β_2 is selected 80° as initial value. Also, in order to obtain a family of solutions, the parameter β_1 can be defined as a range such that from zero to β_2. With the assumed β_1 and β_2 values, the equation set is solved for the vectors $\vec{W}$ and $\vec{Z}$ as below.

For $\beta_2 = 80°$, and $0 < \beta_1 < \beta_2$;

$$\vec{W} = \frac{\begin{vmatrix} \vec{\delta}_1 & e^{i\alpha_1} - 1 \\ \vec{\delta}_2 & e^{i\alpha_2} - 1 \end{vmatrix}}{\begin{vmatrix} e^{i\beta_1} - 1 & e^{i\alpha_1} - 1 \\ e^{i\beta_2} - 1 & e^{i\alpha_2} - 1 \end{vmatrix}} \tag{3.13}$$

$$\vec{Z} = \frac{\begin{vmatrix} e^{i\beta_1} - 1 & \vec{\delta}_1 \\ e^{i\beta_2} - 1 & \vec{\delta}_2 \end{vmatrix}}{\begin{vmatrix} e^{i\beta_1} - 1 & e^{i\alpha_1} - 1 \\ e^{i\beta_2} - 1 & e^{i\alpha_2} - 1 \end{vmatrix}} \tag{3.14}$$

After the solution families for the vectors $\vec{W}$ and $\vec{Z}$ are obtained, the circle points (K) and the center points (M) are calculated and plotted as below. The center and circle points are indicated in black and green in Figure 3.5, respectively.

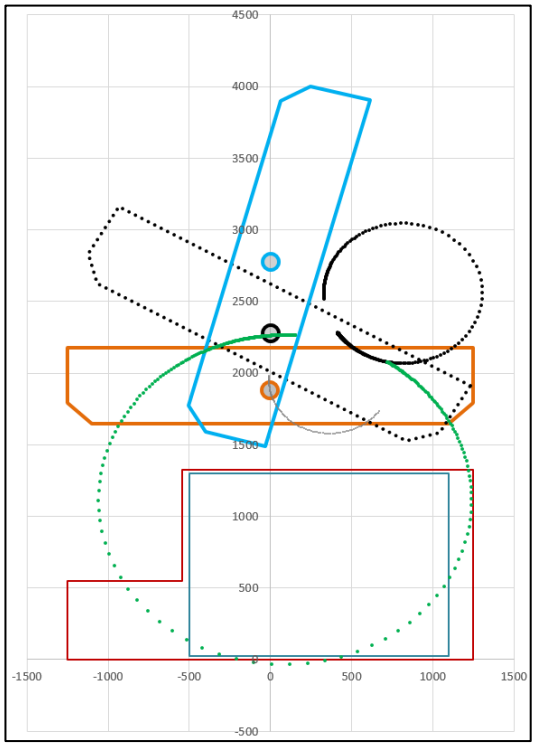

Figure 3.5. Circle and Center Points of the Crank Link

3.2.3.2. The Crank Link for the Desired Fixed Pivot

By considering the obtained solution family for the crank link, the location of the fixed pivot A_0, which mounts the crank link to the chassis, is selected on the chassis with the related design engineer. In order to include the selected fixed pivot to the calculations, the vector $\vec{L}_A$ is defined from the origin to the fixed pivot A_0.

$$\vec{L}_A = 600 + 2100i \tag{3.15}$$

The loop closure equations for the three desired positions are written as below.

$$\vec{W} + \vec{Z} = \vec{R}_1 - \vec{L}_A = \vec{\gamma}_1 \tag{3.16}$$

$$\vec{W}e^{i\beta_1} + \vec{Z}e^{i\alpha_1} = \vec{R}_2 - \vec{L}_A = \vec{\gamma}_2 \tag{3.17}$$

$$\vec{W}e^{i\beta_2} + \vec{Z}e^{i\alpha_2} = \vec{R}_3 - \vec{L}_A = \vec{\gamma}_3 \tag{3.18}$$

The equation set is written in matrix form as below.

$$\begin{bmatrix} 1 & 1 \\ e^{i\beta_2} & e^{i\alpha_2} \\ e^{i\beta_3} & e^{i\alpha_3} \end{bmatrix} \begin{bmatrix} \vec{W} \\ \vec{Z} \end{bmatrix} = \begin{bmatrix} \vec{\gamma}_1 \\ \vec{\gamma}_2 \\ \vec{\gamma}_3 \end{bmatrix} \tag{3.19}$$

To solve the equation set for $\vec{W}$ and $\vec{Z}$, the free parameters β_1 and β_2 can be assumed as specified before. With this approach, the rank of the matrix above becomes two, in other words, the vector pair $\vec{W}$ and $\vec{Z}$ must be linearly dependent to each other. Thus, the following compatibility equation can be written as follow.

$$\begin{vmatrix} 1 & 1 & \vec{\gamma}_1 \\ e^{i\beta_1} & e^{i\alpha_1} & \vec{\gamma}_2 \\ e^{i\beta_2} & e^{i\alpha_2} & \vec{\gamma}_3 \end{vmatrix} = 0 \tag{3.20}$$

By expanding the compatibility equation about the first column, the following equation is obtained.

$$\begin{vmatrix} e^{i\alpha_1} & \vec{\gamma}_2 \\ e^{i\alpha_2} & \vec{\gamma}_3 \end{vmatrix} - e^{i\beta_1} \begin{vmatrix} 1 & \vec{\gamma}_1 \\ e^{i\alpha_2} & \vec{\gamma}_3 \end{vmatrix} + e^{i\beta_2} \begin{vmatrix} 1 & \vec{\gamma}_1 \\ e^{i\alpha_1} & \vec{\gamma}_2 \end{vmatrix} = 0 \tag{3.21}$$

In order to simplify the equation (3.21), the following known vectors are written as below.

$$\vec{\Delta}_1 = \begin{vmatrix} e^{i\alpha_1} & \vec{\gamma}_2 \\ e^{i\alpha_2} & \vec{\gamma}_3 \end{vmatrix} = \vec{\gamma}_3 \times e^{i\alpha_1} - \vec{\gamma}_2 \times e^{i\alpha_2} \tag{3.22}$$

$$\vec{\Delta}_2 = -\begin{vmatrix} 1 & \vec{\gamma}_1 \\ e^{i\alpha_2} & \vec{\gamma}_3 \end{vmatrix} = \vec{\gamma}_1 \times e^{i\alpha_2} - \vec{\gamma}_3 \tag{3.23}$$

$$\vec{\Delta}_3 = \begin{vmatrix} 1 & \vec{\gamma}_1 \\ e^{i\alpha_1} & \vec{\gamma}_2 \end{vmatrix} = \vec{\gamma}_2 - \vec{\gamma}_1 \times e^{i\alpha_1} \tag{3.24}$$

The equation (3.21) is rewritten in terms of the vectors $\vec{\Delta}_i$. $\left(\vec{\Delta}_i, i = 1,2,3\right)$

$$\vec{\Delta}_1 + \vec{\Delta}_2 e^{i\beta_1} + \vec{\Delta}_3 e^{i\beta_2} = 0 \tag{3.25}$$

In order to get rid of the unknown β_1, the equation (3.25) is rearranged as in the equation (3.26), and the conjugate of the equation (3.26) is written in (3.27).

$$\vec{\Delta}_2 e^{i\beta_1} = -\left(\vec{\Delta}_3 e^{i\beta_2} + \vec{\Delta}_1\right) \tag{3.26}$$

$$\overline{\vec{\Delta}_2} e^{-i\beta_1} = -\left(\overline{\vec{\Delta}_3} e^{-i\beta_2} + \overline{\vec{\Delta}_1}\right) \tag{3.27}$$

By multiplying the equations (3.26) and (3.27), the equation is obtained without the unknown β_1.

$$\vec{\Delta}_2 \overline{\vec{\Delta}_2} = \vec{\Delta}_1 \overline{\vec{\Delta}_1} + \vec{\Delta}_3 \overline{\vec{\Delta}_3} + \overline{\vec{\Delta}_1} \vec{\Delta}_3 e^{i\beta_2} + \vec{\Delta}_1 \overline{\vec{\Delta}_3} e^{-i\beta_2} \tag{3.28}$$

All the known terms in the equation (3.28) are collapsed in the defined variable D which is given in (3.29).

$$D = \vec{\Delta}_1 \overline{\vec{\Delta}_1} + \vec{\Delta}_3 \overline{\vec{\Delta}_3} - \vec{\Delta}_2 \overline{\vec{\Delta}_2} \tag{3.29}$$

The equation (3.28) is rewritten as below.

$$\overline{\vec{\Delta}_1} \vec{\Delta}_3 e^{i\beta_2} + \vec{\Delta}_1 \overline{\vec{\Delta}_3} e^{-i\beta_2} + D = 0 \tag{3.30}$$

Then, the equation (3.30) is multiplied by $e^{i\beta_2}$ to obtain a quadratic equation.

$$\overline{\vec{\Delta}_1} \vec{\Delta}_3 e^{i2\beta_2} + D e^{i\beta_2} + \vec{\Delta}_1 \overline{\vec{\Delta}_3} = 0 \tag{3.31}$$

With the definition of the variable t, the quadratic equation (3.31) is written as below.

$$t = e^{i\beta_2} \tag{3.32}$$

$$\overline{\vec{\Delta}_1} \vec{\Delta}_3 t^2 + Dt + \vec{\Delta}_1 \overline{\vec{\Delta}_3} = 0 \tag{3.33}$$

By solving the quadratic equation, the roots t_1 & t_2 are calculated, accordingly β_{2_1} & β_{2_2} are obtained as well. With the availability of the swing angle β_2, the moving pivot of the crank link is calculated as well.

The resultant slider – crank mechanism for the prescribed positions is given in Figure 3.6.

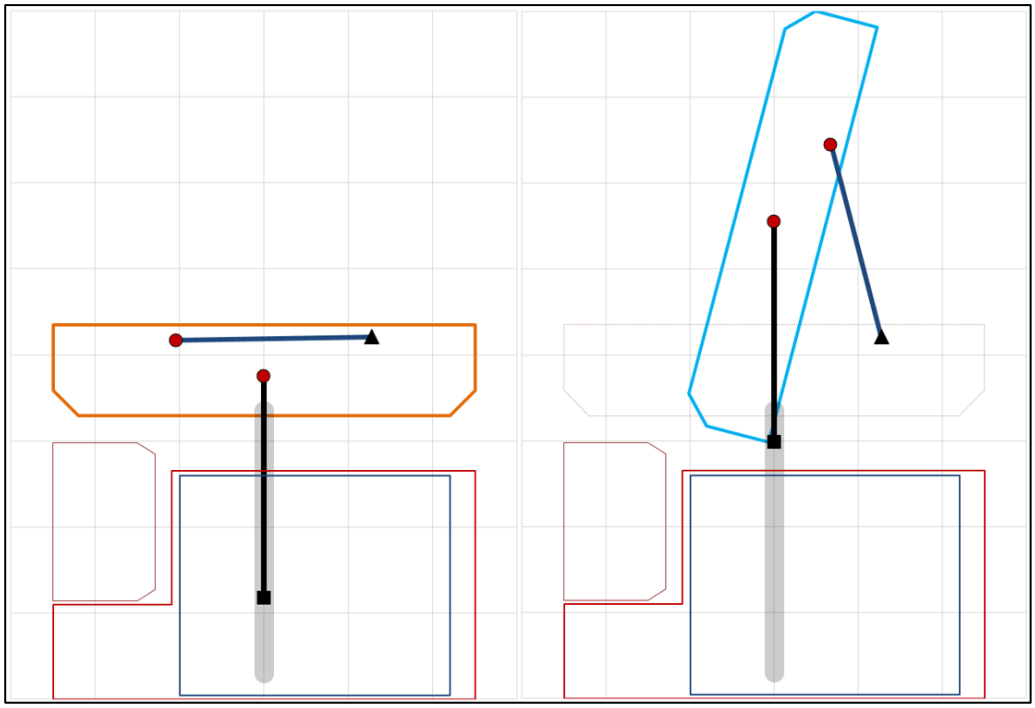

Figure 3.6. The Resultant Slider – Crank Mechanism for A#1

3.3. Kinematic Synthesis of the Mechanism for A#2

According to the selected conceptual mechanism for A#2, the antenna is simply mounted by a hinge on A#1. The location of the pivot B_0 is calculated for the desired positions of A#2 by using Chasles Theorem.

In order to calculate the pivot location accurately, the geometric constraints and desired antenna positions are defined clearly.

3.3.1. Geometric Constraints for A#2

The only geometric restriction for A#2 is that the minimum clearance distance between A#2 and A#1 must be greater than 100 mm during the entire motion. This constraint is defined to provide enough space for the wiring and piping which are used

to transmit electrical power, electronic signal and cooling liquid between A#1 and A#2.

The schematic view of the restricted region is given in Figure 3.7.

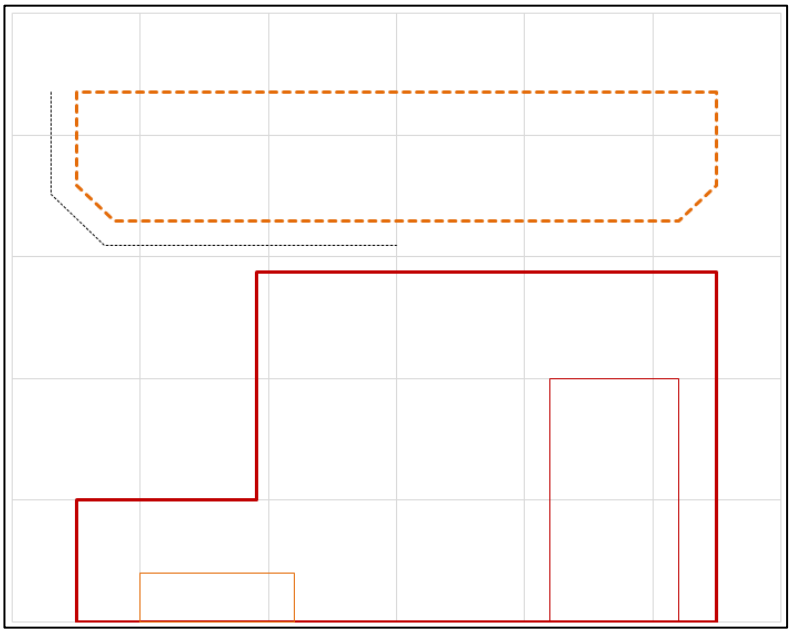

Figure 3.7. The Restricted Region for A#2

3.3.2. Desired Positions of A#2

The locations of A#2 at desired antenna pair positions are not precisely restricted. However, the following requirements must be satisfied at desired positions.

At the transport position, the antenna A#2 must be folded into the permitted volume which is defined by the traffic regulations. Due to the requirement, the bottom face of A#2 is located 140 mm below from the front face of A#1 while the back side of A#2 is aligned with the permitted region. The folded position of A#2 is indicated in orange in Figure 3.8.

At the operating position, the front surface of A#2 must be parallel to the A#1's. Also, the bottom face of A#2 is located 140 mm above the top face of A#1. The operating position of A#2 with respect to A#1 is indicated in blue in Figure 3.8.

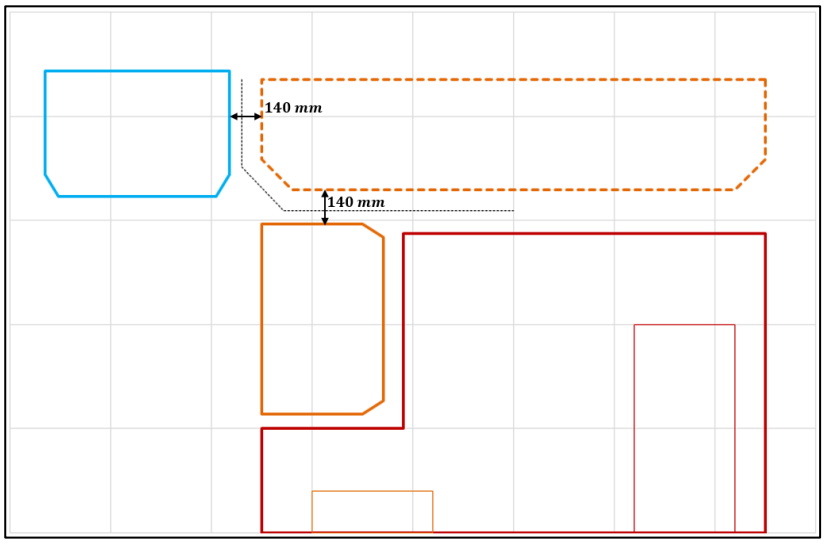

Figure 3.8. Desired Positions of A#2

3.3.3. The Pole for the Desired Positions

Chasles' Theorem specifies that the translation of a rigid body in plane motion can be determined by a pure rotation about the pole alternatively. Based on the Chasles' Theorem, the pole for desired positions is calculated as below. In addition, the used notation for the formula is given in.

$$\vec{P}_{12} = \frac{\vec{a}_2 e^{i\varphi_1} - \vec{a}_1 e^{i\varphi_2}}{e^{i\varphi_1} - e^{i\varphi_2}} \tag{3.34}$$

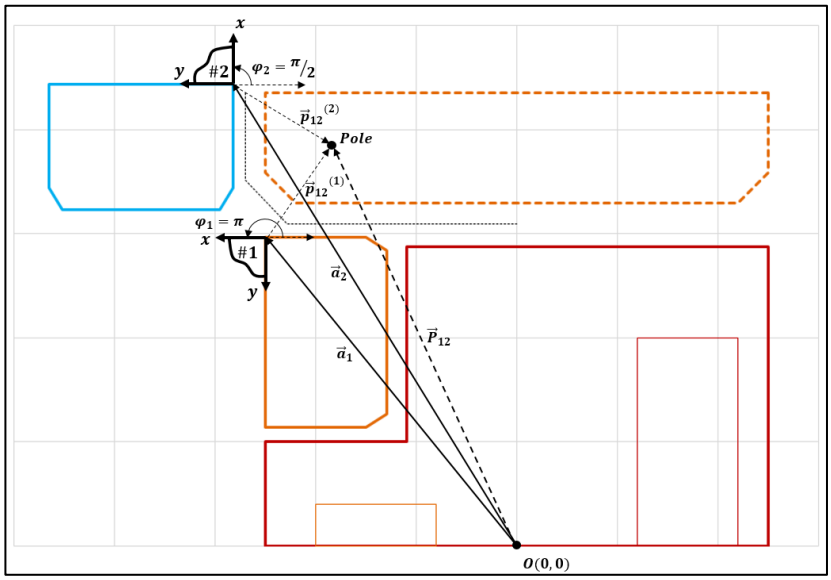

Figure 3.9. The Used Notation for the Pole Calculation

3.4. Relative Motion Synthesis Between A#1 and A#2

By synthesizing an additional four-bar mechanism between the synthesized slider - crank mechanism and A#2, the desired relative motion of A#2 with respect to A#1 is obtained. Thus, the overall folding mechanism will be finalized with 1 DOF as desired.

The synthesis problem for the required four-bar mechanism is known as the correlation of crank angles in the literature. In order to synthesize the required four-bar mechanism analytically, Freudenstein's Equation which is known as the important milestone in modern kinematic is used to define 3 unknown link lengths of the mechanism for 3 desired positions [10][11][12][13]. The used notation for the Freudenstein's Equation is given in Figure 3.10.

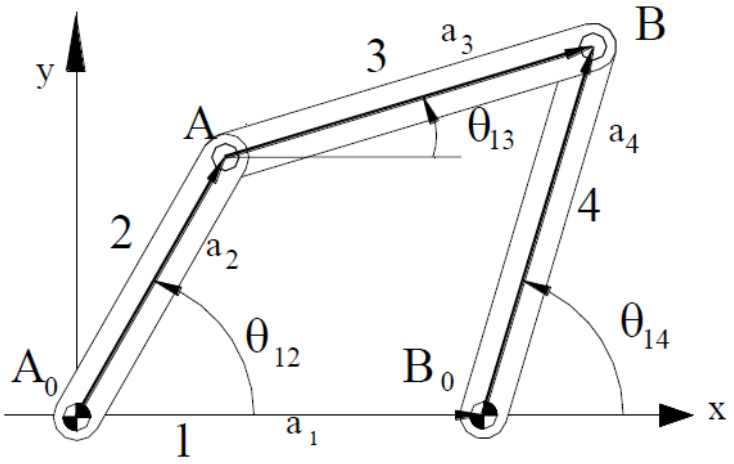

Figure 3.10. The Used Notation of Freduenstein's Equation

The Freudenstein's Equation for the three positions is given in the equation (3.35).

$$K_1 \cos\theta_{14_i} - K_2 \cos\theta_{12_i} + K_3 = \cos\left(\theta_{14_i} - \theta_{12_i}\right); i = 1,2,3 \tag{3.35}$$

Where;

$$K_1 = \frac{a_1}{a_2} \tag{3.36}$$

$$K_2 = \frac{a_1}{a_4} \tag{3.37}$$

$$K_3 = \frac{\left(a_1^{\,2} + a_2^{\,2} - a_3^{\,2} + a_4^{\,2}\right)}{2a_2a_4} \tag{3.38}$$

Since there are two desired positions for the correlation of crank angles, only two linear equations can be written for 3 unknown link lengths. Therefore, there is a free parameter which will be used to optimize the transmission angle. The transmission angle μ is shown in Figure 3.11.

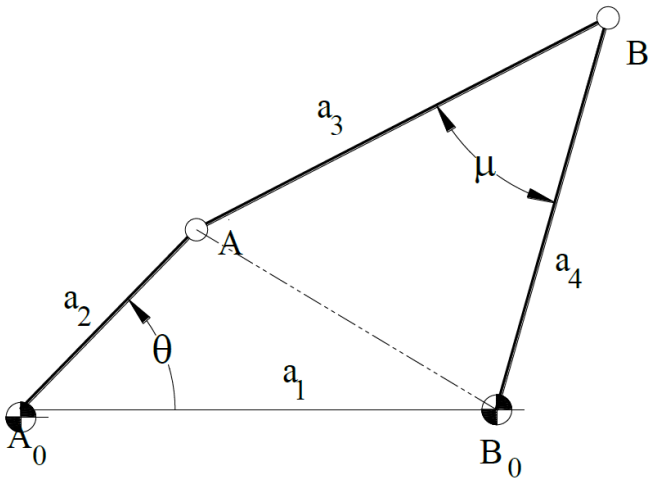

Figure 3.11. The Transmission Angle μ of the Mechanism

The Freduenstein's Equation is written for two positions as below.

$$K_1 \cos\theta_{14_i} - K_2 \cos\theta_{12_i} + K_3 = \cos\left(\theta_{14_i} - \theta_{12_i}\right); i = 1,2 \tag{3.39}$$

In order to include the transmission angle μ to the equation set, cosine theorem is used for the length AB_0.

$$a_1^{\,2} + a_2^{\,2} - 2a_1a_2\cos\theta_{12} = a_3^{\,2} + a_4^{\,2} - 2a_3a_4\cos\mu \tag{3.40}$$

Next, the equation (3.41) is rewritten in terms of the constant parameters K which are defined above.

$$\frac{a_3}{a_2}\cos\mu_i = -K_3 + \frac{K_1}{K_2} + K_2\cos\theta_{12_i}; i = 1,2 \tag{3.41}$$

Based on the foresight that the crank angle θ_{12} will change in range 0 – π or π – 2π, the transmission angle will be maximum and minimum during the transition. If the deviation of the transmission angle from 90°, which is the optimum accessible transmission angle, will be equal at two positions, the transmission angle of the mechanism will have the optimum deviation angle ±δ within the working range.

By assuming the transmission angle $\mu_1 = 90° - \delta$ when $\theta_{12_1} = \theta_0$ and $\mu_1 = 90° + \delta$ when $\theta_{12_2} = \theta_0 + 105°$, the below equation set is written for two positions.

$$\frac{a_3}{a_2}\sin\delta = -K_3 + \frac{K_1}{K_2} + K_2\cos\theta_{12_1} \tag{3.42}$$

$$\frac{a_3}{a_2}\sin\delta = K_3 - \frac{K_1}{K_2} - K_2\cos\theta_{12_2} \tag{3.43}$$

By equating the equations for two positions, the following equation is obtained.

$$K_3 - \frac{K_1}{K_2} + K_2\left(\cos\theta_{12_1} + \cos\theta_{12_2}\right) = 0 \tag{3.44}$$

Lastly, by solving the equations (3.39) and (3.44) together, the link lengths will be obtained for the mechanism which has optimum transmission angle deviation.

3.4.1. Implementation of Freudenstein's Equation

During the transition between transport and an operating position, A#1 rotates by an angle –105° about pivot C with respect to the ground by means of the synthesized slider – crank mechanism. At the same time, A#1 rotates about pivot C with respect to the slider link of the mechanism as well. Since the mechanism will provide the required relative motion of A#2 on A#1, the mechanism is synthesized on the moving body A#1. Therefore, the inverse motion theory is used.

Based on the inverse motion theory, the slider link rotates by an angle +105° about pivot C with respect to A#1 during the transition. On the other hand, A#2 rotates by an angle –90° about the pivot B_0 as studied in the previous section. The changes of input and output link angles for two positions are given in Figure 3.12.

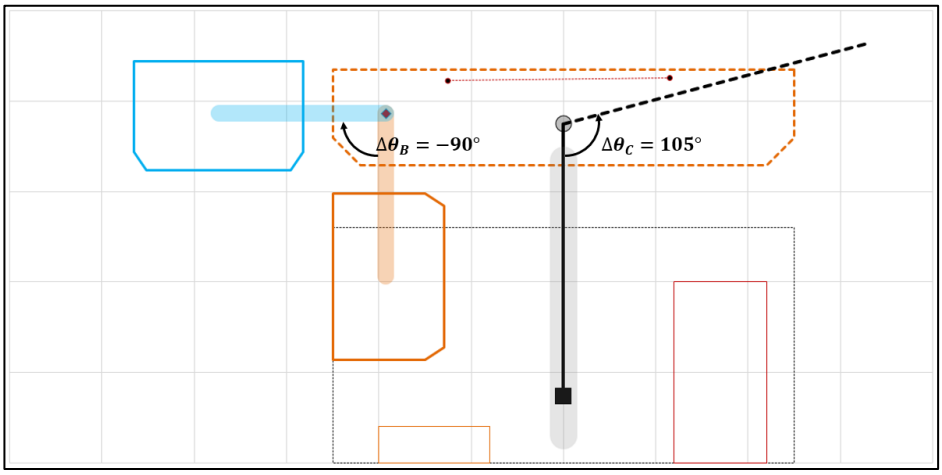

Figure 3.12. The Deviations of Input and Output Link Angles

In order to define two positions for the correlation of crank angles, desired crank angles are defined as below. Initial crank angles θ_{B_1} and θ_{C_1} are free parameters that will be defined on the problem sketch by considering geometric restrictions. Also, the crank angles θ_{B_2} and θ_{C_2} for the second position are calculated as below.

$$\theta_{B_2} = \theta_{B_1} - 90° \tag{3.45}$$

$$\theta_{C_2} = \theta_{C_1} + 105° \tag{3.46}$$

Then, the equations (3.39) and (3.44) are implemented to the problem as below.

$$K_1 \cos\theta_{B_1} - K_2 \cos\theta_{C_1} + K_3 = \cos\left(\theta_{B_1} - \theta_{C_1}\right) \tag{3.47}$$

$$K_1 \cos\theta_{B_2} - K_2 \cos\theta_{C_2} + K_3 = \cos\left(\theta_{B_2} - \theta_{C_2}\right) \tag{3.48}$$

$$K_3 - \frac{K_1}{K_2} + K_2\left(\cos\theta_{C_1} + \cos\theta_{C_2}\right) = 0 \tag{3.49}$$

By solving the equation set, link lengths of the mechanism are calculated for the desired motion. In Figure 3.13, the obtained mechanism is given for both positions. The free initial crank angles are selected approximately by considering the outline of the antenna system.

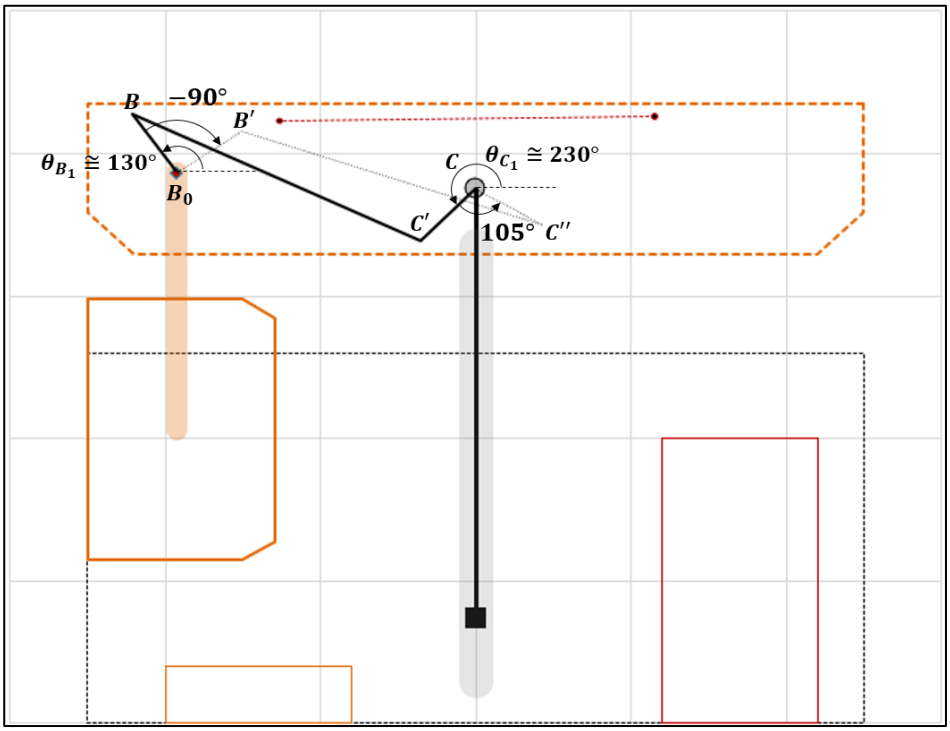

Figure 3.13. The Resultant Mechanism for the Desired Relative Motion

3.5. Kinematic Analysis of the Mechanism

After synthesis study is completed for the mechanism, the next step is performing kinematic analysis to obtain the entire motion of the mechanism between desired positions.

As a first step, joint variables and link constants are represented symbolically for future analytic derivations. The joint variables are illustrated in the mechanism in Figure 3.14.

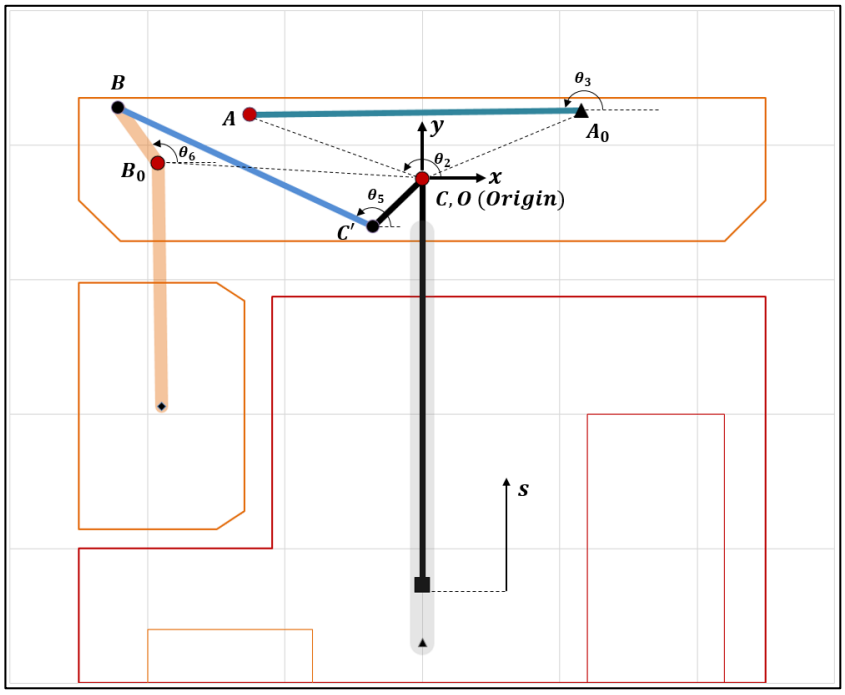

Figure 3.14. The Schematic Representation of the Joint Variables

Additionally, the constant link lengths are represented as below.

$$
\begin{aligned}
a_1 &= |OA_0| \\
a_2 &= |AC| \\
a_3 &= |A_0A| \\
a_4 &= |CC'| \\
a_5 &= |C'B| \\
a_6 &= |B_0B| \\
a_7 &= |CB_0|
\end{aligned}
\tag{3.50}
$$

$$
\begin{aligned}
\gamma_1 &= \angle xOA_0 \\
\gamma_2 &= \angle ACB_0 \\
\gamma_4 &= \angle xCC'
\end{aligned}
\tag{3.51}
$$

Since the synthesized mechanism is a single degree of freedom mechanism, the stroke (s) of the point C is the input joint variable of the entire mechanism. Also, the other dependent joint variables are calculated as depended on the joint variable s.

On the other hand, the mechanism consists of two independent mechanism chains. Therefore, two loop closure equations should be written and solved in order. The first loop closure can be written for the slider-crank portion of the mechanism with respect to the joint variable s.

$$\overrightarrow{OC} + \overrightarrow{CA} = \overrightarrow{OA_0} + \overrightarrow{A_0A} \tag{3.52}$$

$$is + a_2 e^{i\theta_2} = a_1 e^{i\gamma_1} + a_3 e^{i\theta_3} \tag{3.53}$$

By solving the vector equation (3.53), the unknown joint variables θ_2 and θ_3 can be found as below.

$$\theta_2 = \arctan_2\left(A_x, A_y\right) + \arccos\left(B\right) \tag{3.54}$$

$$\theta_3 = \arctan_2\left(C_x, C_y\right) \tag{3.55}$$

Where;

$$A_x = a_1 \cos\gamma_1 \tag{3.56}$$

$$A_y = a_1 \sin\gamma_1 - s \tag{3.57}$$

$$B = \frac{{a_2}^2 + \left(a_1 \cos\gamma_1\right)^2 + \left(a_1 \sin\gamma_1 - s\right)^2 - {a_3}^2}{2a_2\sqrt{\left(a_1 \cos\gamma_1\right)^2 + \left(a_1 \sin\gamma_1 - s\right)^2}} \tag{3.58}$$

$$C_x = a_2 \cos\theta_2 - a_1 \cos\gamma_1 \tag{3.59}$$

$$C_y = s + a_2 \sin\theta_2 - a_1 \sin\gamma_1 \tag{3.60}$$

With the availability of the joint variable θ_2, the second loop is written for the four-bar mechanism portion of the mechanism.

$$\overrightarrow{CC'} + \overrightarrow{C'B} = \overrightarrow{CB_0} + \overrightarrow{B_0B} \tag{3.61}$$

$$a_4 e^{i\gamma_4} + a_5 e^{i\theta_5} = a_7 e^{i(\theta_2 + \gamma_2)} + a_6 e^{i\theta_6} \tag{3.62}$$

By solving the vector equation (3.62), the unknown joint variables θ_5 and θ_6 can be found as below.

$$\theta_6 = \arctan_2\left(D_x, D_y\right) + \arccos\left(E\right) \tag{3.63}$$

$$\theta_5 = \arctan_2\left(F_x, F_y\right) \tag{3.64}$$

Where;

$$D_x = a_4 \cos\gamma_4 - a_7 \cos\left(\theta_2 + \gamma_2\right) \tag{3.65}$$

$$D_y = a_4 \sin\gamma_4 - a_7 \sin\left(\theta_2 + \gamma_2\right) \tag{3.66}$$

$$E = \frac{{a_6}^2 + {G_x}^2 + {G_y}^2 - {a_5}^2}{2a_6\sqrt{{G_x}^2 + {G_y}^2}} \tag{3.67}$$

$$F_x = -G_x + a_6 \cos\theta_6 \tag{3.68}$$

$$F_y = G_y + a_6 \sin\theta_6 \tag{3.69}$$

$$G_x = a_4 \cos\gamma_4 - a_7 \cos\left(\theta_2 + \gamma_2\right) \tag{3.70}$$

$$G_y = a_4 \sin\gamma_4 - a_7 \sin\left(\theta_2 + \gamma_2\right) \tag{3.71}$$

After all, the motion of the mechanism can be analyzed for desired stroke values by means of the obtained equations for the joint variables $\theta_2, \theta_3, \theta_5$ and θ_6. As a first step, the swept region is examined in terms of the interference and the clearance with the restricted region by performing position analysis.

According to the requirements, the first significant restriction is that the antenna pair should not interfere with the region which is allocated for the cooling units under A#1. As mentioned in 3.2.2, the second A#1 position is defined arbitrarily to control the swept region during the transition. By changing the second pose of A#1, the swept region is translated above the allocated region.

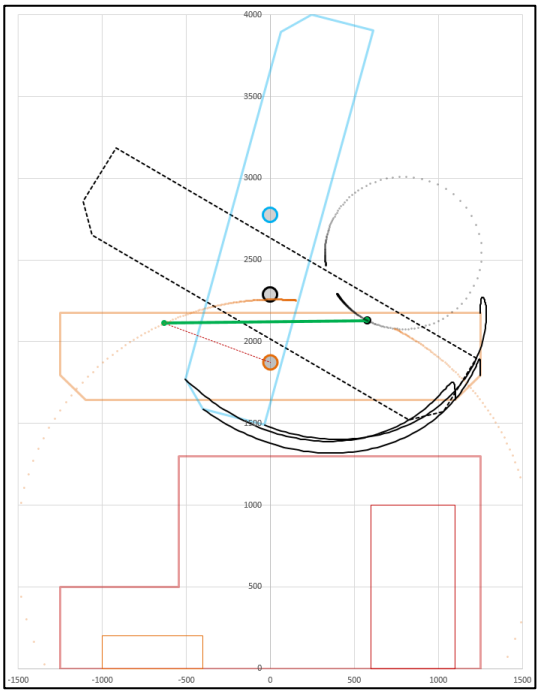

Figure 3.15. The Swept Region by A#1

The other important interference possibility that is the minimum distance between the A#2 and A#1 should be greater than 100 mm for the piping and wiring, is also analyzed. As seen in Figure 3.16, the desired clearance between the antenna pair is satisfied during the motion.

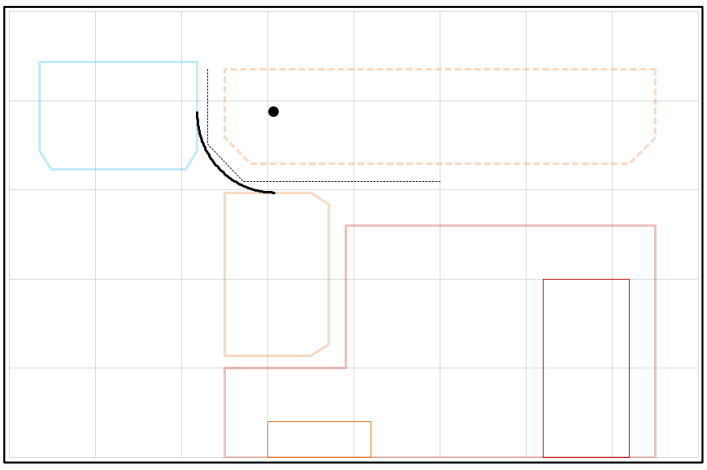

Figure 3.16. The Desired Clearance Between the Antenna Pair

Additionally, the entire motion of the mechanism is also analyzed in order to check the desired antenna positions. All desired positions are given respectively in Figure 3.17.

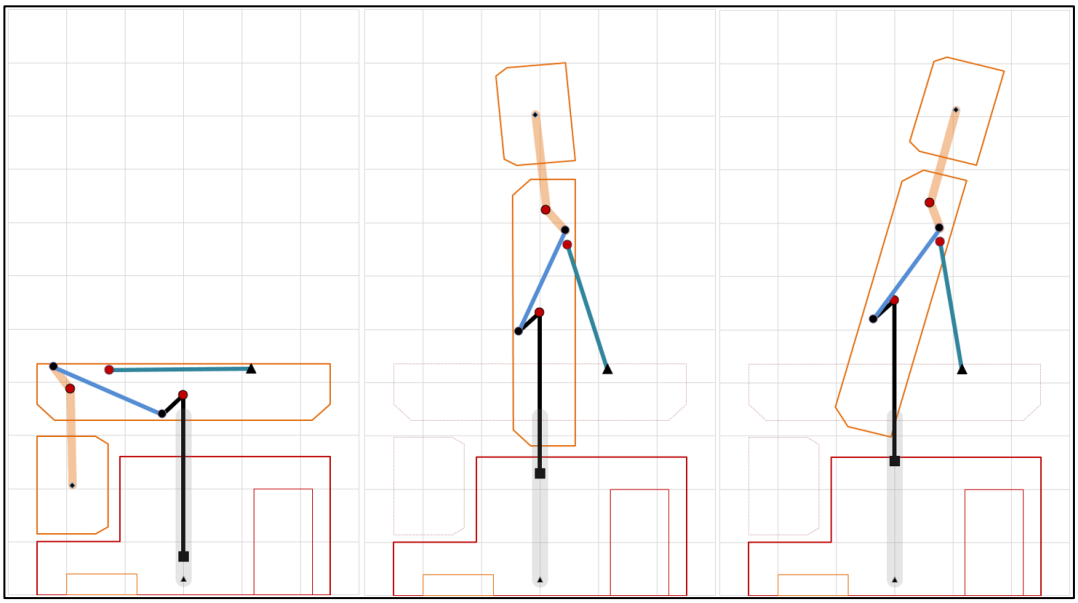

Figure 3.17. The Developed Folding Mechanism at Desired Antenna Positions

Lastly, due to the given transition time at requirements, the motion of the folding mechanism is quite slow. Therefore, only position analysis is performed for the mechanism.

3.6. Force Analysis of the Mechanism

In order to obtain the driving force of the mechanism which is applied to the input link, a quasi-static force analysis is performed on the mechanism by neglecting all inertial forces. Furthermore, all bearing forces should be calculated for future mechanical design stage. Therefore, Newton – Euler approach is used instead of the virtual work method to obtain all structural reaction forces of the mechanism at the same time.

During calculations, the masses of links are neglected since their weights are very small when compared to antenna pair. Since the slider link is the main carrier of the system, its mass cannot be neglected. Therefore, a quasi-static analysis is proceeded by adding the assumed mass value of the sliders to the A#1's. At the end of the study, the assumption will be compared with the real physical properties of the system.

3.6.1. External Forces

The first step of the force analysis is defining the exposed external forces clearly. As expected, the weights of the antenna pair are the most significant portion of the system. Since the exact center of gravity locations of antennas are not known, the geometric centers of antennas are assumed as the center of gravity for each antenna initially.

On the other hand, the exposed wind load is also critical for the system. In order to define the wind loads accurately, Computational Fluid Dynamics (CFD) analysis is performed for the various antenna positions between desired positions for the wind speed at ±162 km/h along the horizontal direction. For this study, a simple 3D model is created for the system. In Figure 3.18, the resultant flow curves at the position of A#1 at 15° is given as an example. Also, the calculated wind loads on antennas for different positions are given in Figure 3.19 and Figure 3.20. The resultant force values are used in calculations by fitting polynomials on obtained force values with a scale factor.

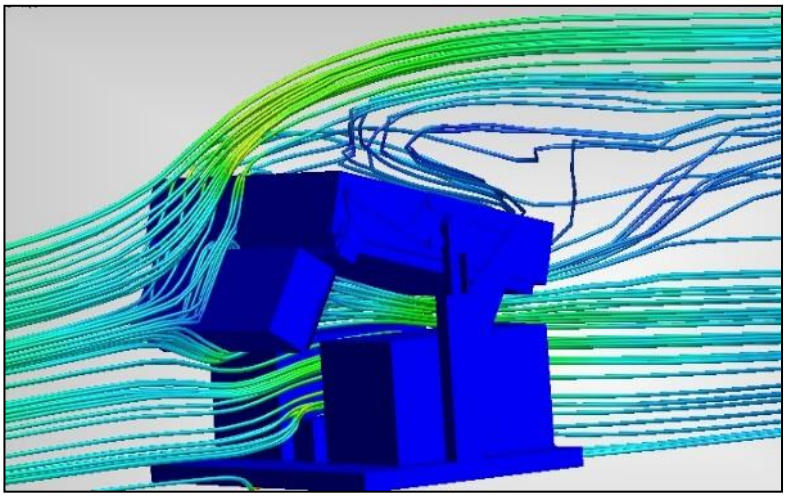

Figure 3.18. The Resultant Flow Curves at 15°

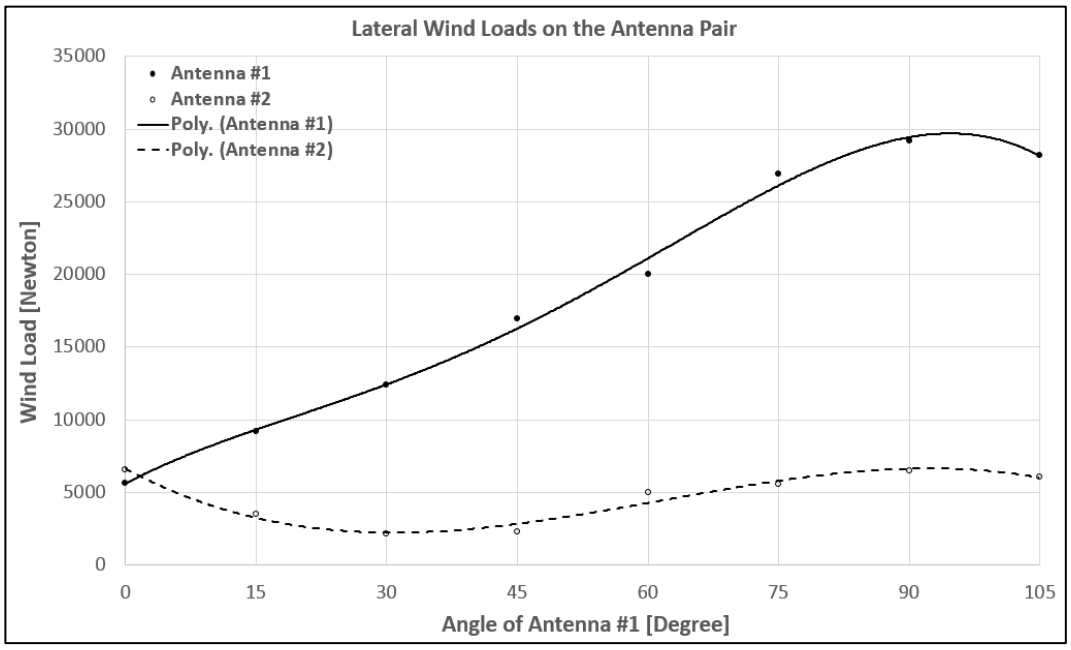

Figure 3.19. The Resultant Lateral Wind Forces on the Antenna Pair

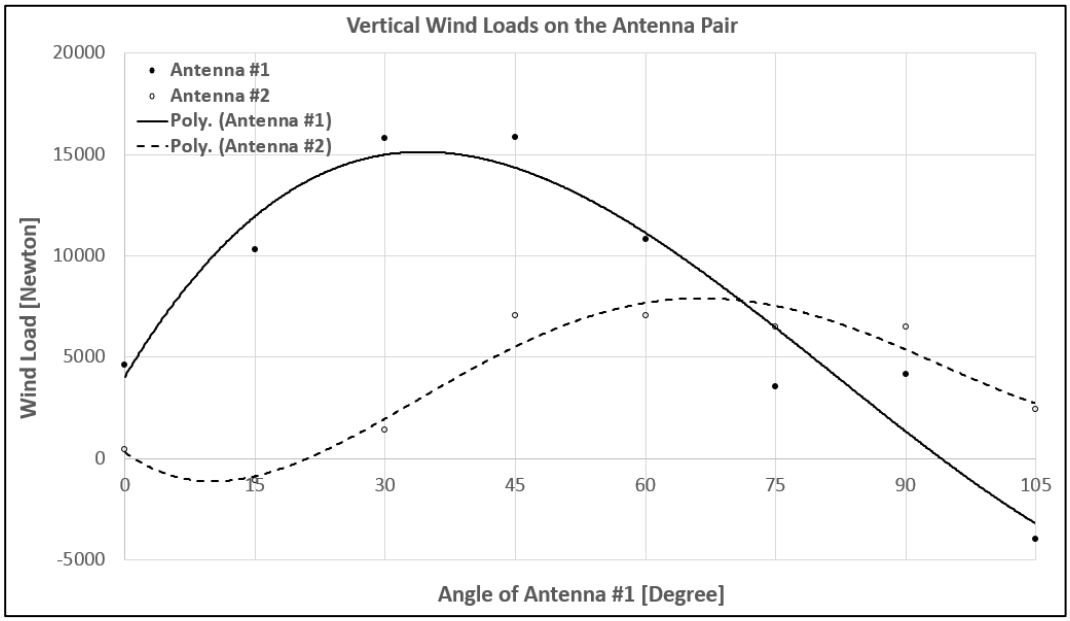

Figure 3.20. The Resultant Vertical Wind Forces on the Antenna Pair

All external forces are shown on the mechanism in Figure 3.21.

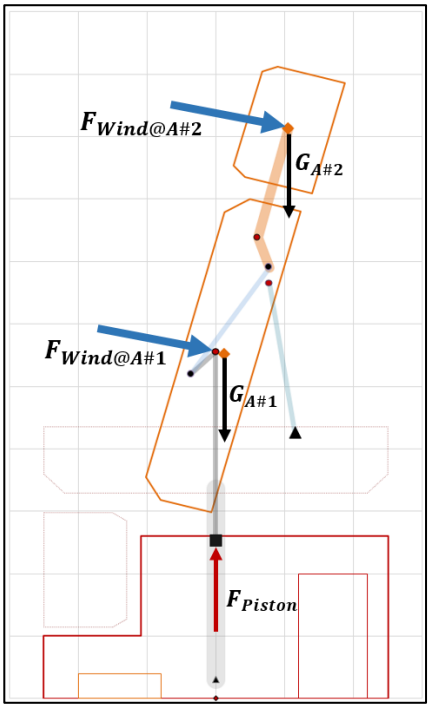

Figure 3.21. All External Forces on the Mechanism

3.6.2. Free Body Diagrams

After all external forces on the system are defined, the next step is determining the free body diagram of each link. Free body diagrams of links are given in detail as follow.

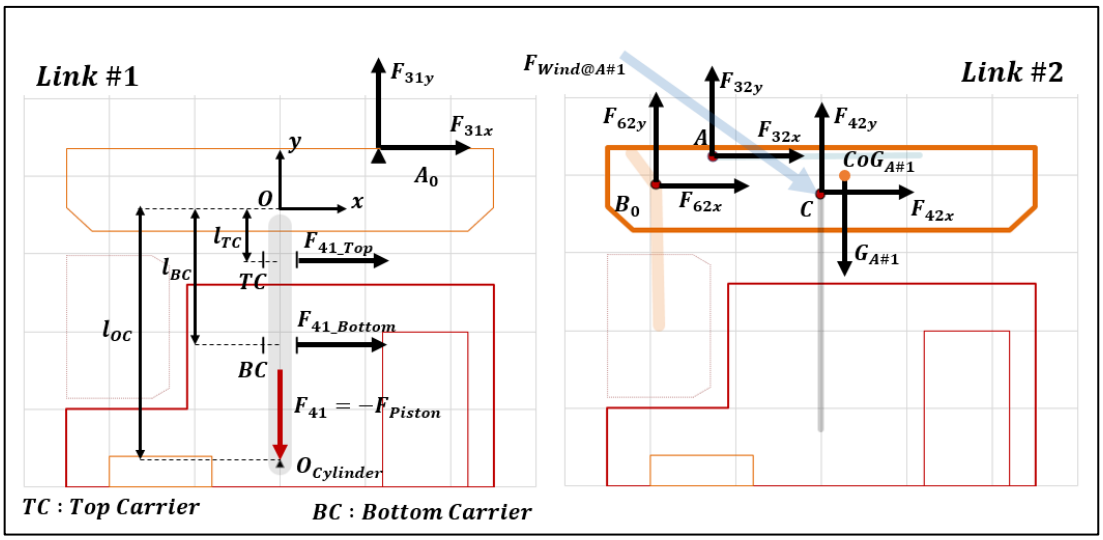

Figure 3.22. Free Body Diagrams of the Link 1 and 2

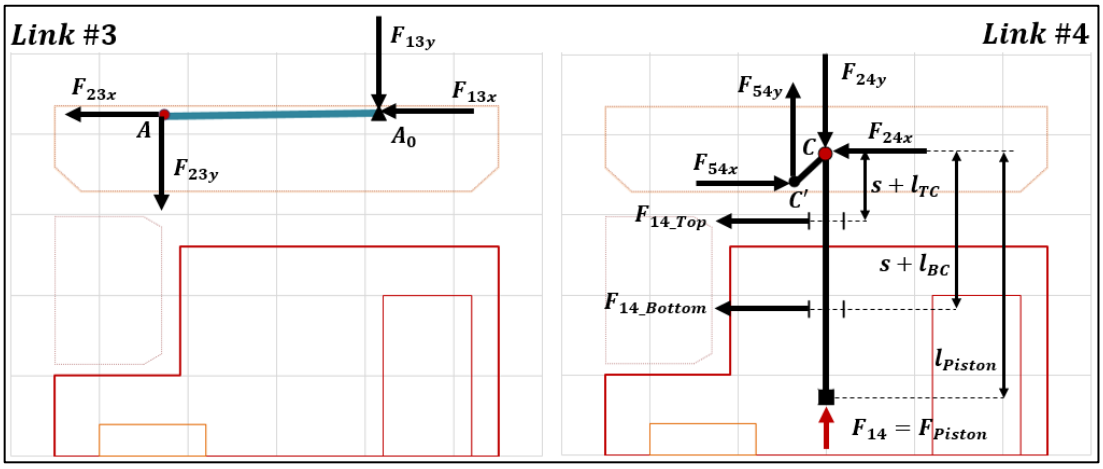

Figure 3.23. Free Body Diagrams of the Link 3 and 4

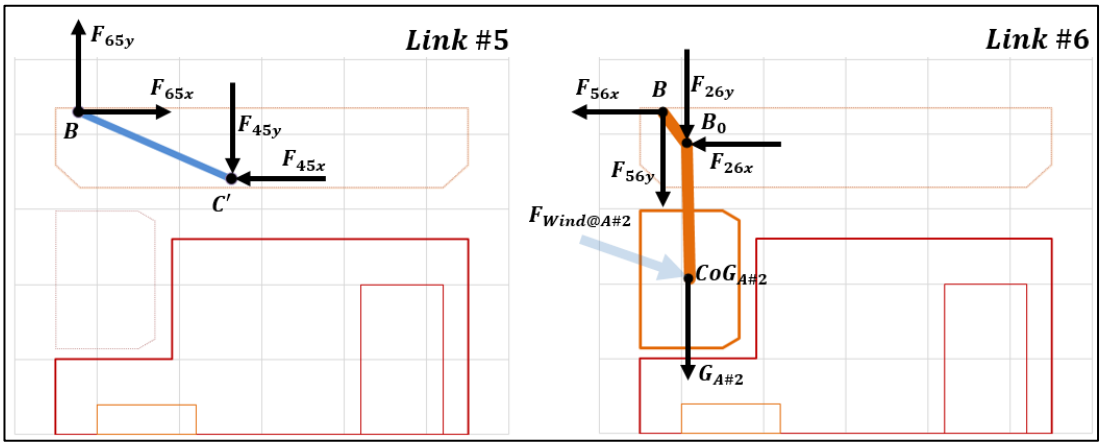

Figure 3.24. Free Body Diagrams of the Link 5 and 6

It is important to note that joint forces will be equal but in the opposite direction which bases on the 3rd law of Newton. Therefore, the following relationship is used in calculations.

$$\vec{F}_{ij(x,y)} = -\vec{F}_{ji(x,y)} \tag{3.72}$$

$$\left|\vec{F}_{ij(x,y)}\right| = \left|\vec{F}_{ji(x,y)}\right| \tag{3.73}$$

3.6.3. Equilibrium Equations

In order to calculate the unknown joint forces, the force and moment equilibrium equations are written with respect to the free body diagrams of links which are obtained at the previous section.

The following 15 equilibrium equations are written for the Link #2, #3, #4, #5 and #6.

$$\sum \vec{F}_x = \vec{0} \tag{3.74}$$

$$\sum \vec{F}_y = \vec{0} \tag{3.75}$$

$$\sum \vec{M} = \vec{0} \tag{3.76}$$

By solving the equation set, the 15 scalar unknowns F_{piston}, F_{12x}, F_{12y}, F_{14_T}, F_{14_B}, F_{23x}, F_{23y}, F_{24x}, F_{24y}, F_{26x}, F_{26y}, F_{45x}, F_{45y}, F_{56x} and F_{56y} are calculated.

Additionally, since the slider link (Link #4) is mounted on the chassis (Link #1) by a slider – carrier components, the friction forces on carriers which occur because of the

forces F_{14_T} and F_{14_B}, should be included to calculations. In order to calculate the friction forces with respect to friction coefficient μ which can be found in the datasheet of the product, the Coulomb Friction Theory is used.

$$\vec{F}_{Friction} = -\mu \times \left(\left| \vec{F}_{14\_T} \right| + \left| \vec{F}_{14\_B} \right| \right) \times sign(\dot{s}) \tag{3.77}$$

Also, the total piston force can be calculated as below.

$$\vec{F}_{Piston\_Total} = \vec{F}_{Piston} + \vec{F}_{Friction} \tag{3.78}$$

Lastly, all calculations are derived for a planar mechanism. Since the synthesized mechanism will be placed at two sides of the antenna pair, the calculated joint forces should be divided by two to size links and select components.

3.7. Balancing of the Mechanism

Since the mass of the antenna pair is quite high, a balancing study may offer a significant improvement on the joint and driving forces of the mechanism. Instead of adding additional balancing masses on the mechanism, a wisely antenna placement by adjusting the center of gravities of antennas may provide the same improvement. Therefore, the mechanism is analyzed in this respect.

As a first step of the study, the motion of the center of gravities and the calculated driving force are examined. In Figure 3.25, the mechanism is analyzed for the assumed CoG locations which are defined at geometric centers of antennas. As seen in the figure, the path of the $CoG_{A\#1}$ seems a vertical straight line during the motion. In other words, the $CoG_{A\#1}$ goes up as much as the stroke against the gravity. Therefore, a huge change in potential energy between the desired positions is required for the system. On the other hand, an enormous change in the path of $CoG_{A\#1}$ along the vertical direction is an unavoidable fact. Consequently, the calculated total piston force requirement for the assumed CoG locations is given in Figure 3.26 as well.

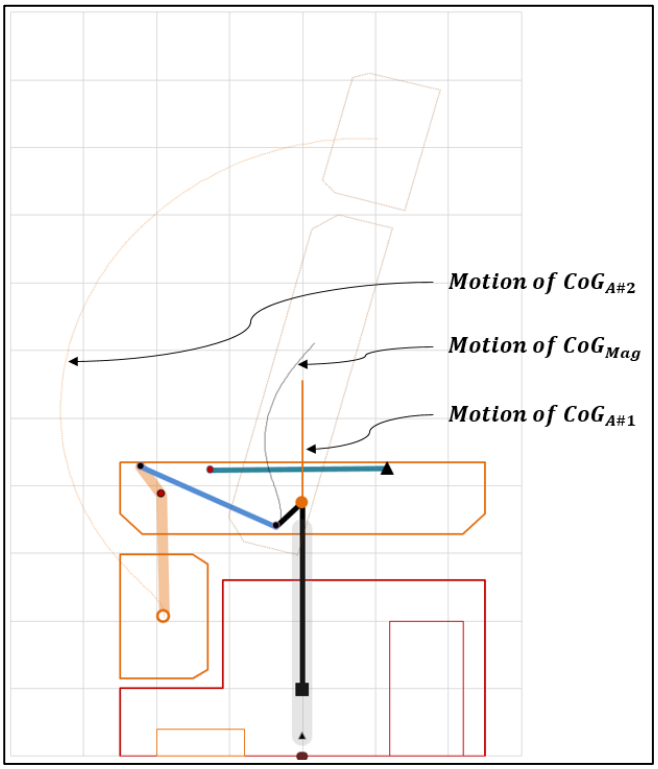

Figure 3.25. The Motions of Assumed CoG Locations

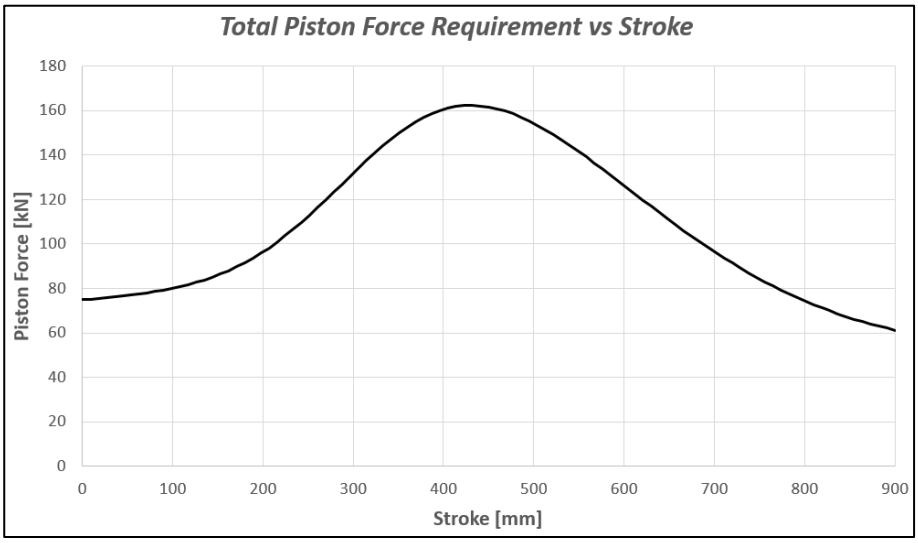

Figure 3.26. The Total Force Requirement for the Assumed CoG Locations

If the motion of antennas about the pivot C is investigated carefully, it is quite easy to see that the antenna pair rotates by an angle –105° about the pivot C during the motion. Since the $CoG_{A\#1}$ is located on the pivot C, the weight of A#1 does not create a moment about the pivot C. But, if the $CoG_{A\#1}$ will be located at the other side of the pivot C, the $CoG_{A\#1}$ goes down with the help of the gravity. Thereby, the weight of the A#1 helps to the mechanism to lift A#2 up. In order words, the antenna pair can be balanced with each other without additional mass. Although it is not possible to balance the antenna pair completely, this approach will only provide as much improvement as possible. The explained balancing study on the mechanism is given in Figure 3.27.

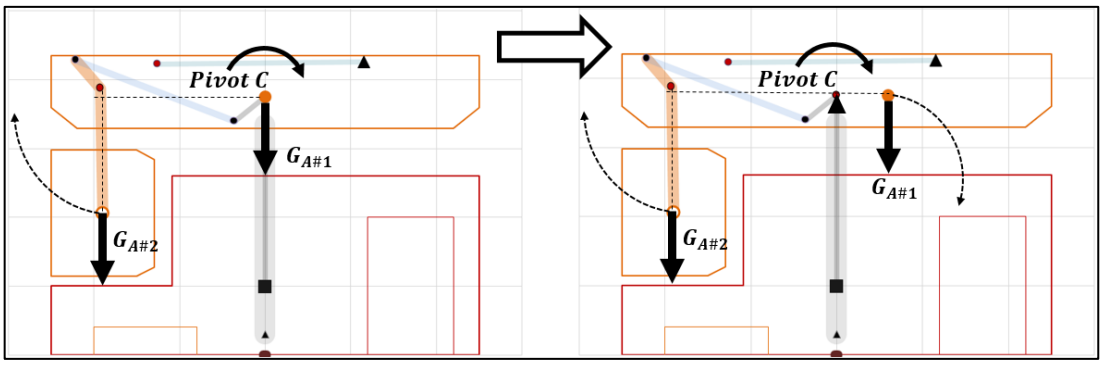

Figure 3.27. The Balancing Study on the Mechanism

On the other hand, an important point must be considered in the balancing study is that the $CoG_{A\#1}$ should not pass to the other side during the motion. Otherwise, the $CoG_{A\#1}$ will go up against the gravity. Therefore, the angle of the line, which is between the $CoG_{A\#1}$ and the pivot C, with the horizontal axis should be greater than 15°.

By discussing with the design engineer of A#1, the region of achievable $CoG_{A\#1}$ locations is determined. The determined region is indicated by a rectangular in Figure 3.28.

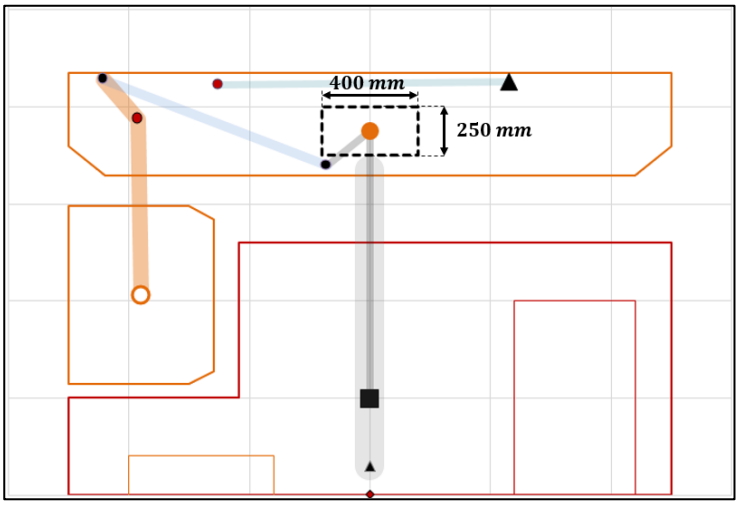

Figure 3.28. The Region of Achievable CoG Locations

Then, an optimization study is performed in order to find the optimum $CoG_{A\#1}$ location in terms of the balanced antenna pair within the determined region. The generalized reduced gradient (GRG) method is preferred which is embedded ready-to-use code in Excel® for the optimization study. In the optimization study, the objective function is defined as the minimization of the maximum piston force value. Also, the $CoG_{A\#1}$ location is defined as the variable with the constraints which are defined with respect to the determined achievable region.

At the end of the optimization study, the right top corner of the region, which is the farthest location to pivot C, is found as the optimum location for the minimum piston force requirement. Indeed, the result is a quite predictable with respect to the previous analysis studies. The optimized $CoG_{A\#1}$ location and the motions of all CoG locations are given in Figure 3.29.

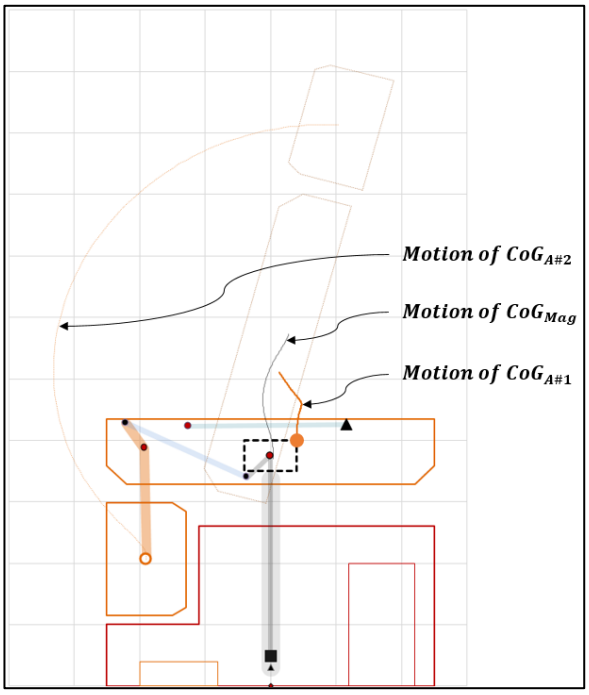

Figure 3.29. The Motions of Optimized CoG Location

Additionally, the calculated piston force for the optimized $CoG_{A\#1}$ location is given in as well. As seen in the figure, the balancing study provides a significant improvement in the piston force requirement that is almost %25 less than the previous.

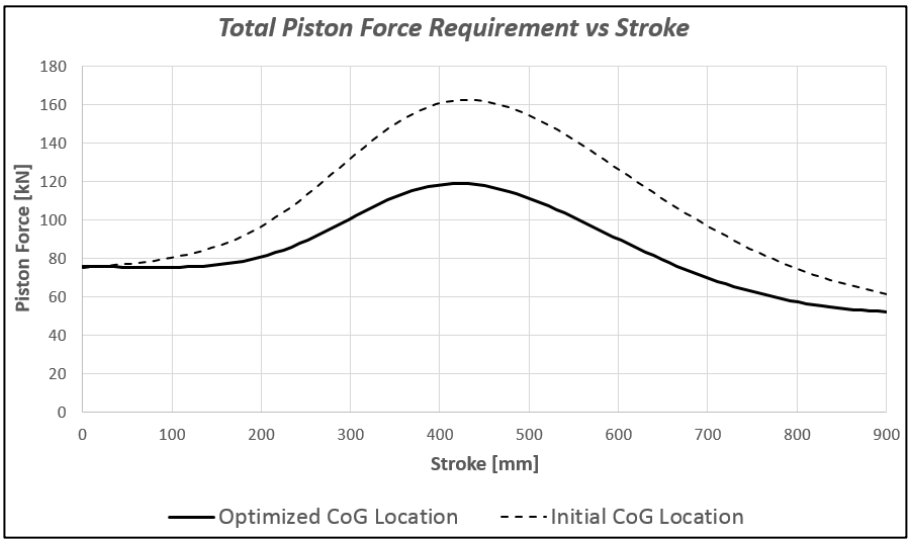

Figure 3.30. The Total Force Requirement for the Optimized CoG Location

Consequently, the adjustment of the CoG at a desired position exactly may not be easy in such a big antenna in real life. However, through this study, the ideal $CoG_{A\#1}$ location in terms of balancing is identified, and it can be aimed as much as possible in the design phase.

CHAPTER 4

IMPLEMENTATION OF THE MECHANISM

4.1. Introduction

In this chapter, the implementation of the developed mechanism to the real system is presented. As a first step of the implementation study, all joint forces, which are obtained by the performed force analysis, are examined. According to the exposed forces, the off-the-shelf products are selected for the joints, and the links are sized roughly. Then, each part of the assembly is shaped and assembled in a CAD program.

After a 3D model is obtained for the system, detailed strength and modal analyses are performed on the system by using the Finite Element Method (FEM). By taking the analyses results into account, the shapes of links are finalized. Additionally, the usage of locking mechanisms is evaluated in order to improve the rigidity of the system.

Note that, since the system is quite big and complicated, the detailed and finalized mechanical design of the entire system for manufacturing is not aimed in the scope of the thesis. Therefore, this chapter only provides the necessary section dimensions of the links in terms of the required strength and rigidity.

4.2. Embodiment of the Design

As a first step of the embodiment study, the off – the – shelf components are selected with respect to the exposed joint forces which are obtained at the previous section. Since the motion of the system is quite low, only static loads are considered for the component selection. The nomenclature of the pivots is given in Figure 4.1.

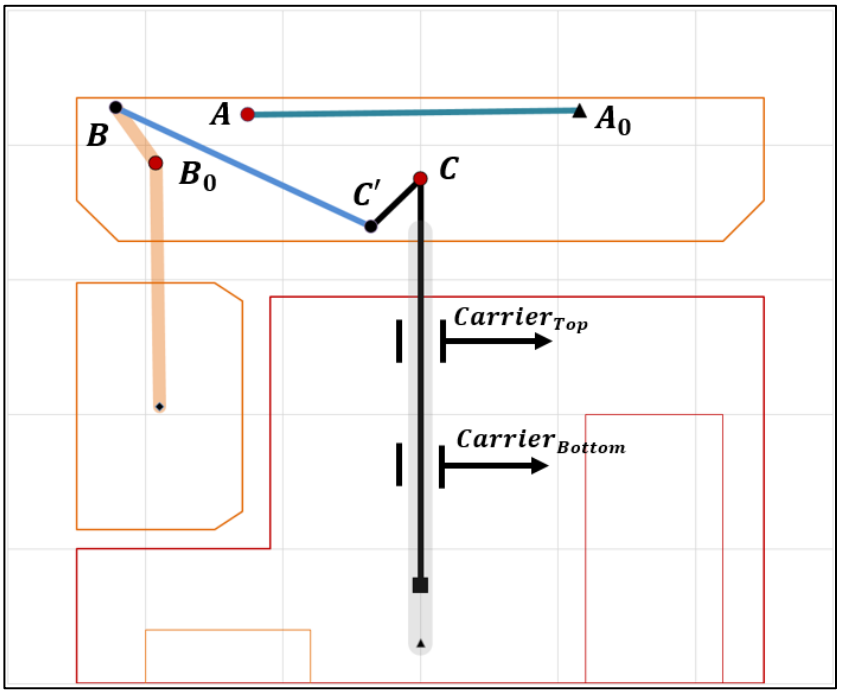

Figure 4.1. The Nomenclature of the Pivots

In Table 1, the absolute maximum values of the exposed loads during the transition are given below.

Table 4.1. *The Calculated Joint Forces*

Pivot	$F_{\max}\,[kN]$
A_0	60
A	60
B_0	45
B	35
C	125
C’	35
$Carrier_{Top}$	185
$Carrier_{Bottom}$	185

On the other hand, the used electromechanical actuators are specially developed for the project with respect to the force and stroke requirement of the mechanism.

In addition to selecting components from the market, the loads are also taken into consideration while sizing the links. After selecting off – the – shelf components, the links are shaped with respect to the selected components and exposed loads. Link #5 and #6, which work as a two forces member, are easily sized by analytical methods with respect to the physical properties of the selected AISI 316 stainless steel material.

On the other hand, since the other links are exposed to three joint forces, an analytical approach cannot be performed easily. With respect to some assumptions and simplifications on the boundary conditions for each link, the links are sized as possible. However, the sizes and shapes of links are examined and improved in terms of strength and stiffness during the FEM analyses which are performed iteratively. AL 5083 material is selected for the rest of the parts.

After sizing the links according to the exposed loads, each part is shaped and assembled in Siemens NX® CAD software. In Figure 4.2, the view of the generated 3D model for the radar system at the operating position is shown. In addition, the view of the 3D model at the transport position is given in Figure 4.3.

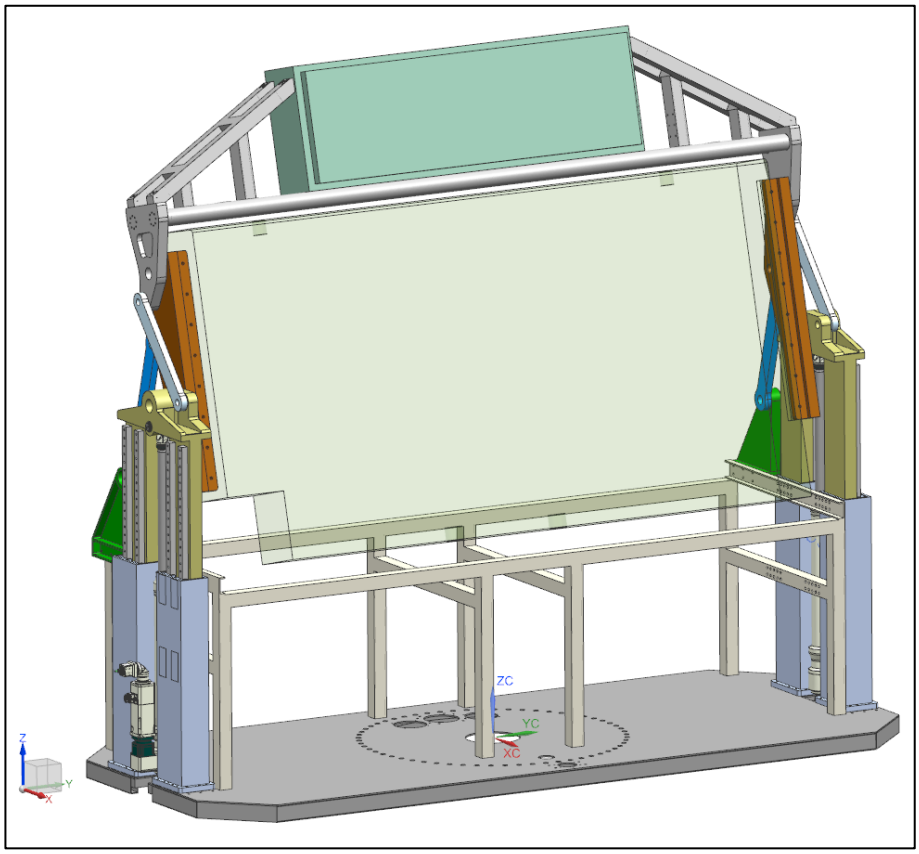

Figure 4.2. The 3D Model of the Simplified Radar System at the Operating Position

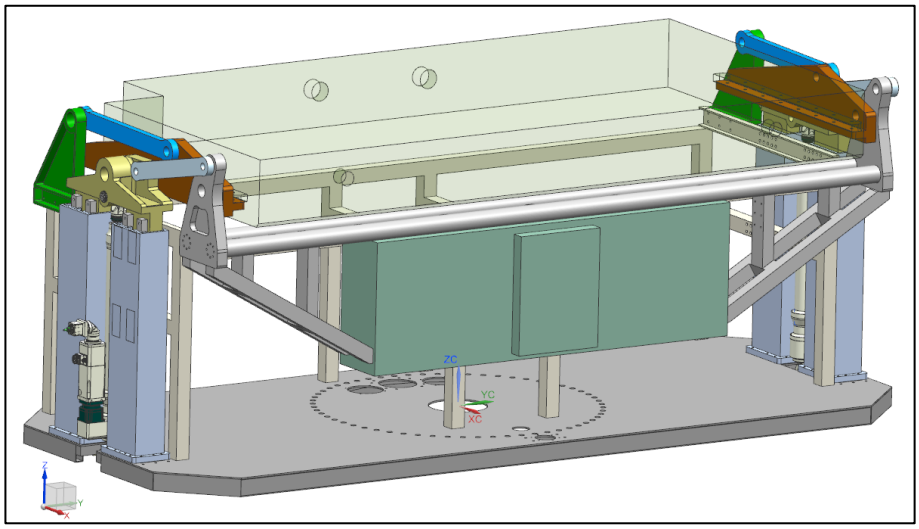

Figure 4.3. The 3D Model of the Simplified Radar System at the Transport Position

4.3. Simulation Studies

In order to design the folding mechanism with necessary rigidity and strength, simulation studies are iteratively performed on the 3D model of the system during the design phase.

As a first step of simulation studies, finite element analyses are performed on the system to check the natural frequencies and the strength of the design at the operating position. MSC Nastran®, which is the commercial FEA solver, is used for finite element analyses. Then, in order to check the strength of the system during the entire motion, a flexible MBD analysis is performed on the system by using Craig – Bampton Method in MSC Adams®. In the light of the simulation results, sizes of the links are improved to achieve desired rigidity and strength. Additionally, the results of the quasi-static analysis which is performed analytically at the previous chapter are validated.

4.3.1. Finite Element Analyses

Firstly, a finite element model is created with necessary boundary conditions based on the types of the used joints. The created finite element model for the final design is given in Figure 4.4.

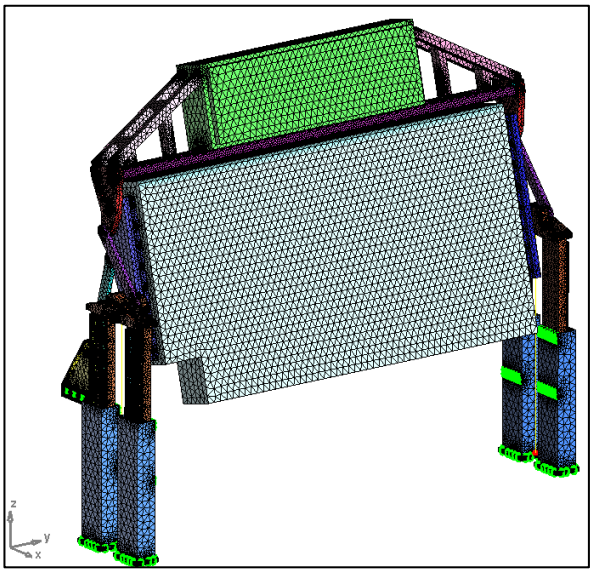

Figure 4.4. The Created Finite Element Model for the Design

After the finite element model is created, a modal analysis is performed in order to obtain the natural frequencies of the system at the operating position. In addition to the frequency values, the calculated mode shapes are also examined to interpret the behavior the system at the resonance frequencies. The calculated natural frequency values for the first ten resonance modes of the system are given in Table 4.2.

Table 4.2. *The Natural Frequencies of the System*

Mode Number	Frequency [Hz]
1	6.61
2	10.16
3	13.45
4	22.20
5	25.27
6	34.59
7	43.67
8	52.24
9	52.99
10	58.92

Besides, the mode shapes of the first ten resonance modes of the system are given respectively in Figure 4.5 and Figure 4.6.

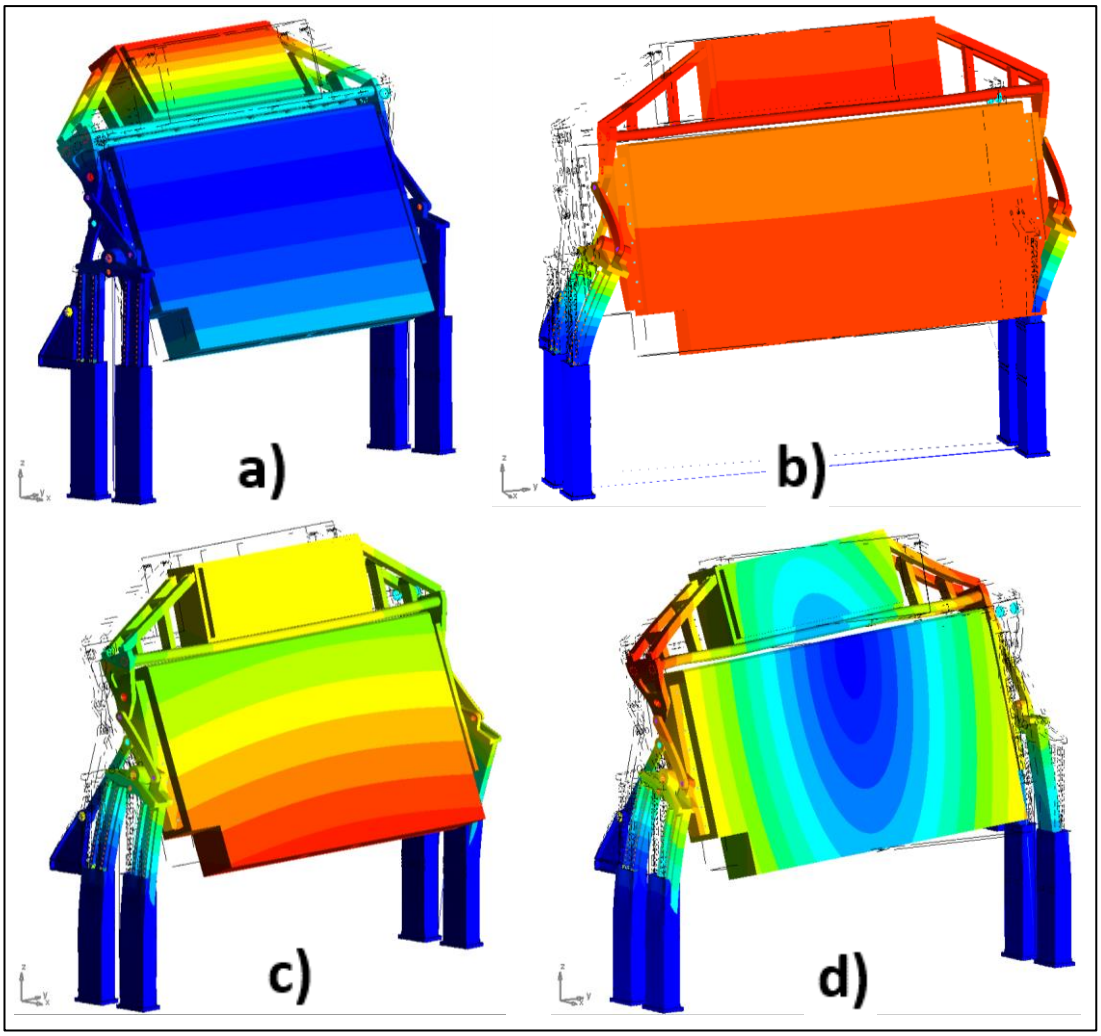

Figure 4.5. a) First Mode Shape b) Second Mode Shape c) Third Mode Shape d) Fourth Mode Shape

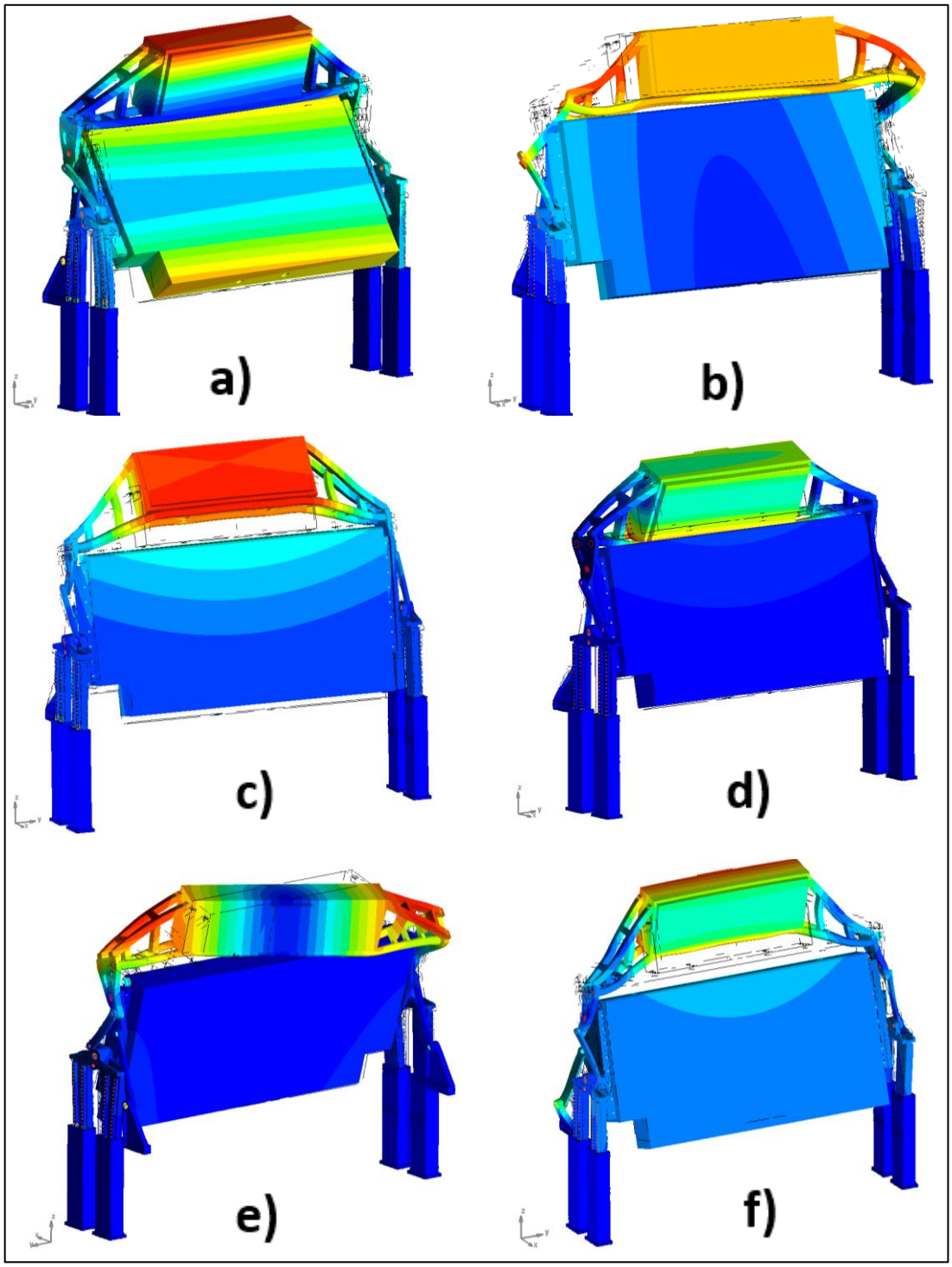

Figure 4.6. . a) Fifth Mode Shape b) Sixth Mode Shape c) Seventh Mode Shape d) Eighth Mode Shape e) Ninth Mode Shape g) Tenth Mode Shape

In addition to the modal analysis, the strength of the system is investigated under gravity and the wind load by performing static analysis. Resulting stresses and displacements on the system are given in Figure 4.7 and Figure 4.8.

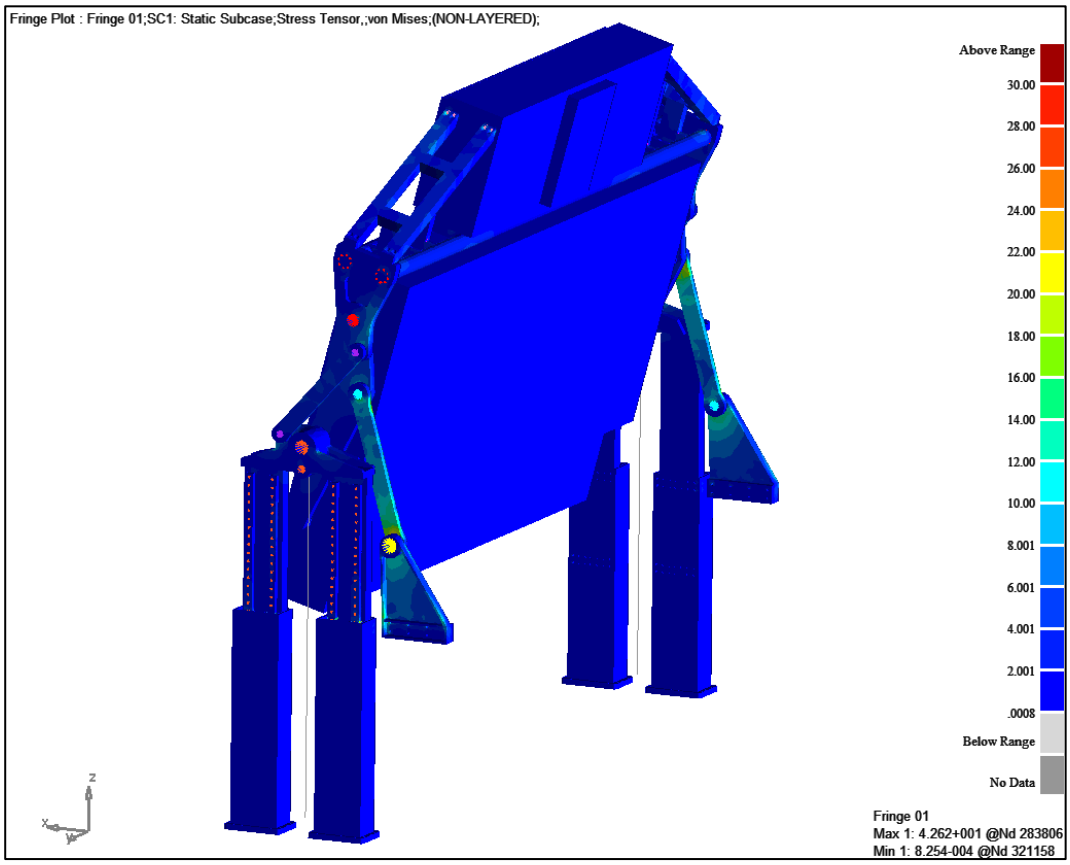

Figure 4.7. The Von Misses Stresses on the System

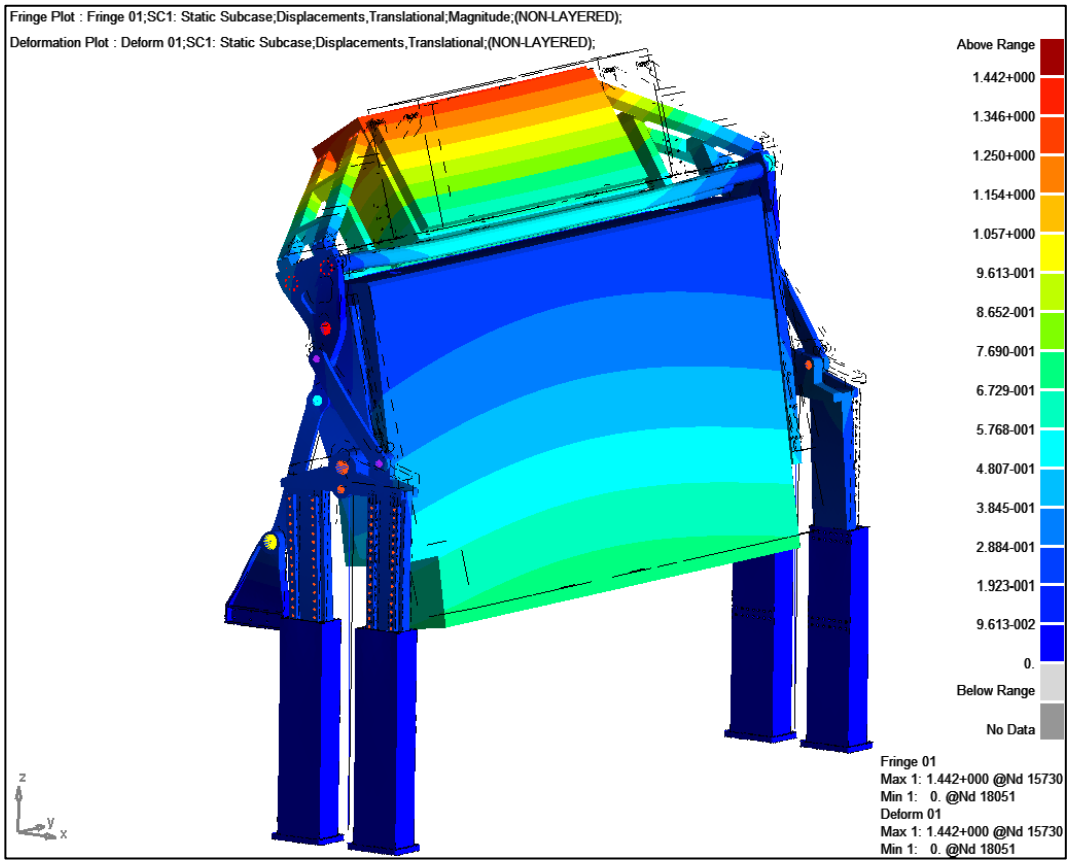

Figure 4.8. The Displacement of the System with the Exaggerated Deformation

As seen in Figure 4.7, the stresses on links are quite low with respect to the yield stresses of the materials. However, the system is exposed to the high joint forces during the transition between desired positions. In other words, higher stresses occur on the mechanism during movement. Therefore, a flexible MBD analysis is performed for the entire motion of the system to obtain the maximum stress value of the system that occurs during the transition.

On the other hand, by investigating the mode shapes of the system, it is clearly seen that most of the resonance modes are almost appeared as the rigid body modes of the antenna pair. In other words, the structure of the designed folding mechanism is not stiff enough to hold the antenna pair rigidly. Therefore, two locking mechanisms are designed between the antenna pair and the chassis. The first locking mechanism pair is placed on the chassis of A#2, and the piston of the mechanism extends into the

chassis of A#1 at the operating position. The other locking mechanism pair is placed on the main chassis to lock A#1 to chassis in the same way. All locking mechanisms restrict the relative motion between the related parts along the radial directions. The designed locking mechanisms are given in Figure 4.9.

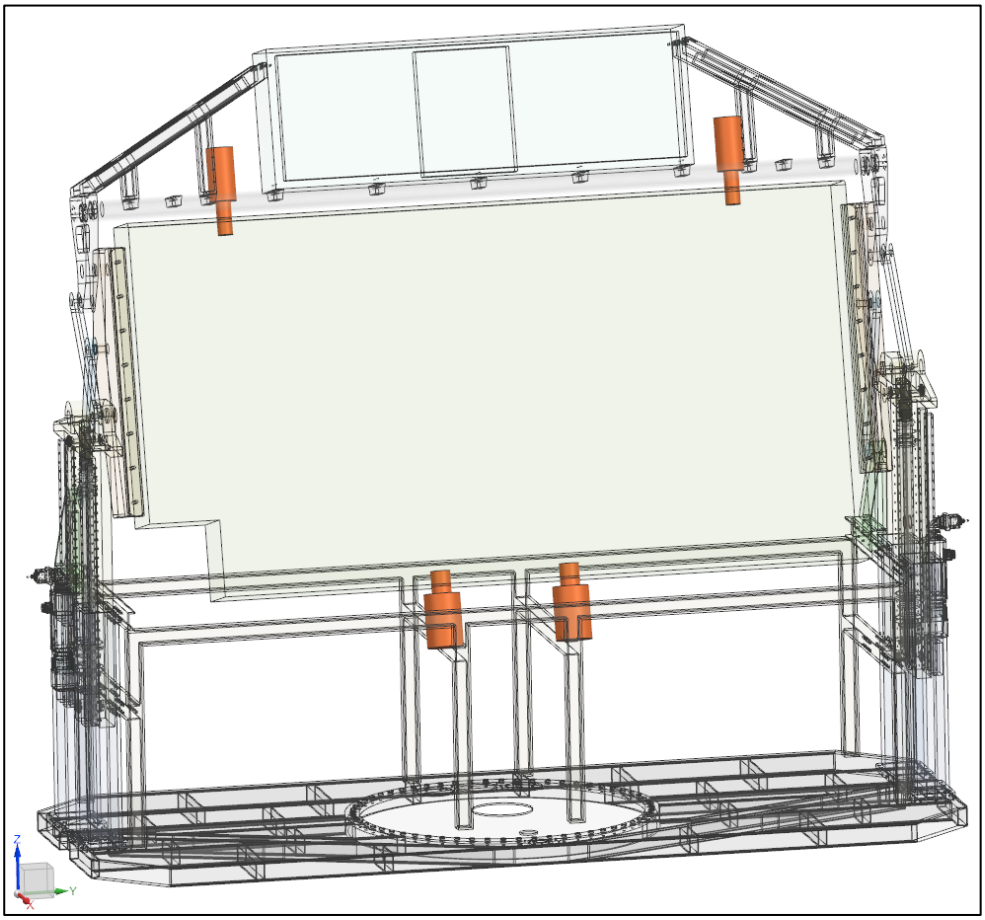

Figure 4.9. The Designed Locking Mechanisms

In order to see the effects of the locking mechanisms, the modal and static analyses are repeated for the locked antenna configuration. With respect to the 3D model of the system, the locking mechanisms are added to the existing finite element model to restrict the relative motion between the related parts along the radial directions.

The natural frequencies of the locked antenna configuration are given with previous results in Table 4.3. As seen in table, the resonance frequencies of the system increased significantly due to the locking mechanisms.

Table 4.3. *The Natural Frequencies of the Locked Antenna Configuration*

Mode Number	Initial Configuration Frequency [Hz]	Locked Antenna Configuration Frequency [Hz]
1	6.61	17.70
2	10.16	38.01
3	13.45	39.72
4	22.20	51.26
5	25.27	59.29
6	34.59	65.17
7	43.67	78.65
8	52.24	79.87
9	52.99	80.21
10	58.92	96.40

Besides, the mode shapes of the first four resonance modes of the system at locked antenna configuration are given in Figure 4.10.

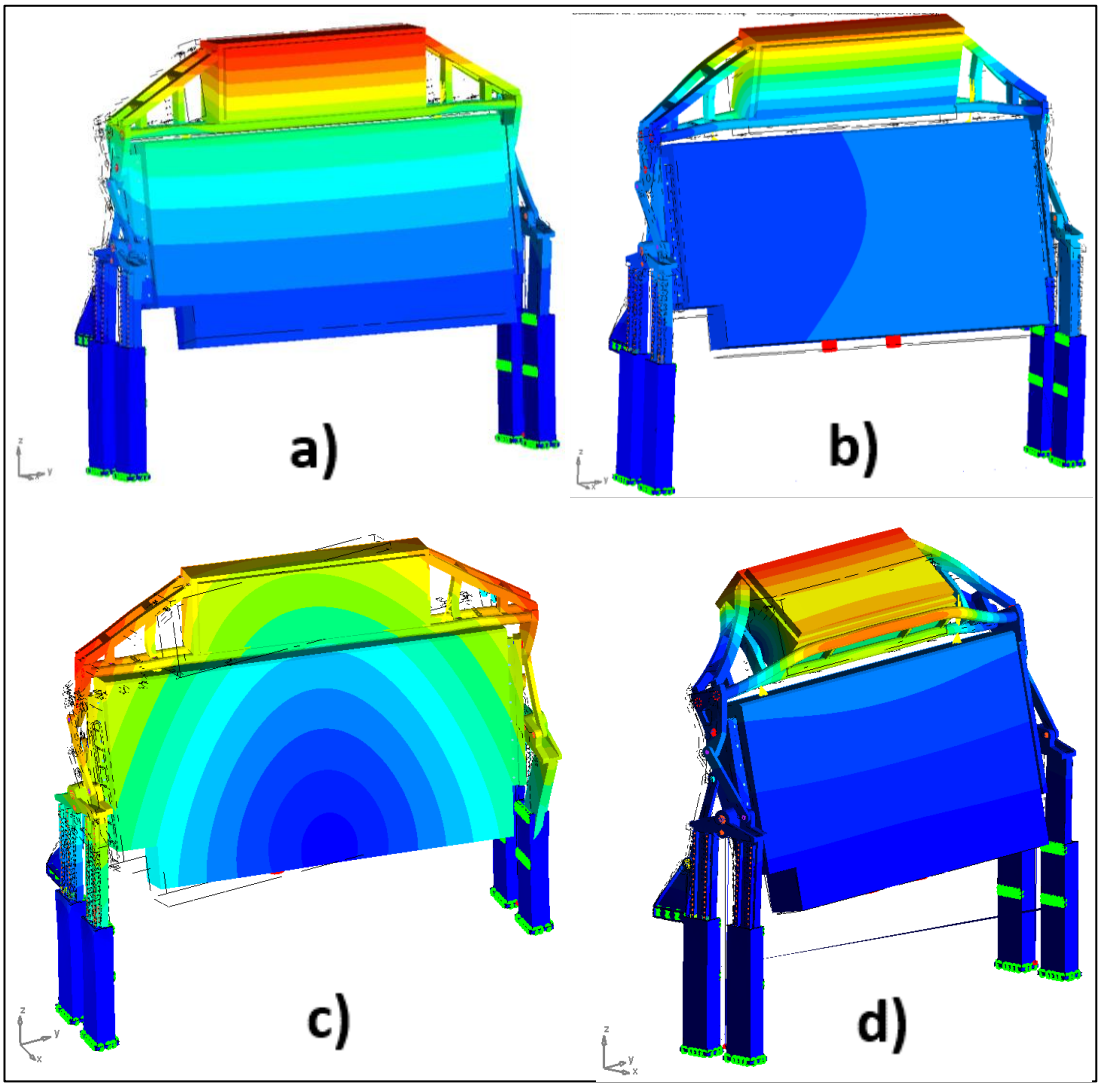

Figure 4.10. a) First Mode Shape b) Second Mode Shape c) Third Mode Shape d) Fourth Mode Shape

Lastly, the deformation of the system at locked antenna configuration is reanalyzed under the exposed wind load and gravity. As seen in Figure 4.11, the maximum displacement of the system is reduced to 0.6 mm which is an acceptable deformation at the operating position.

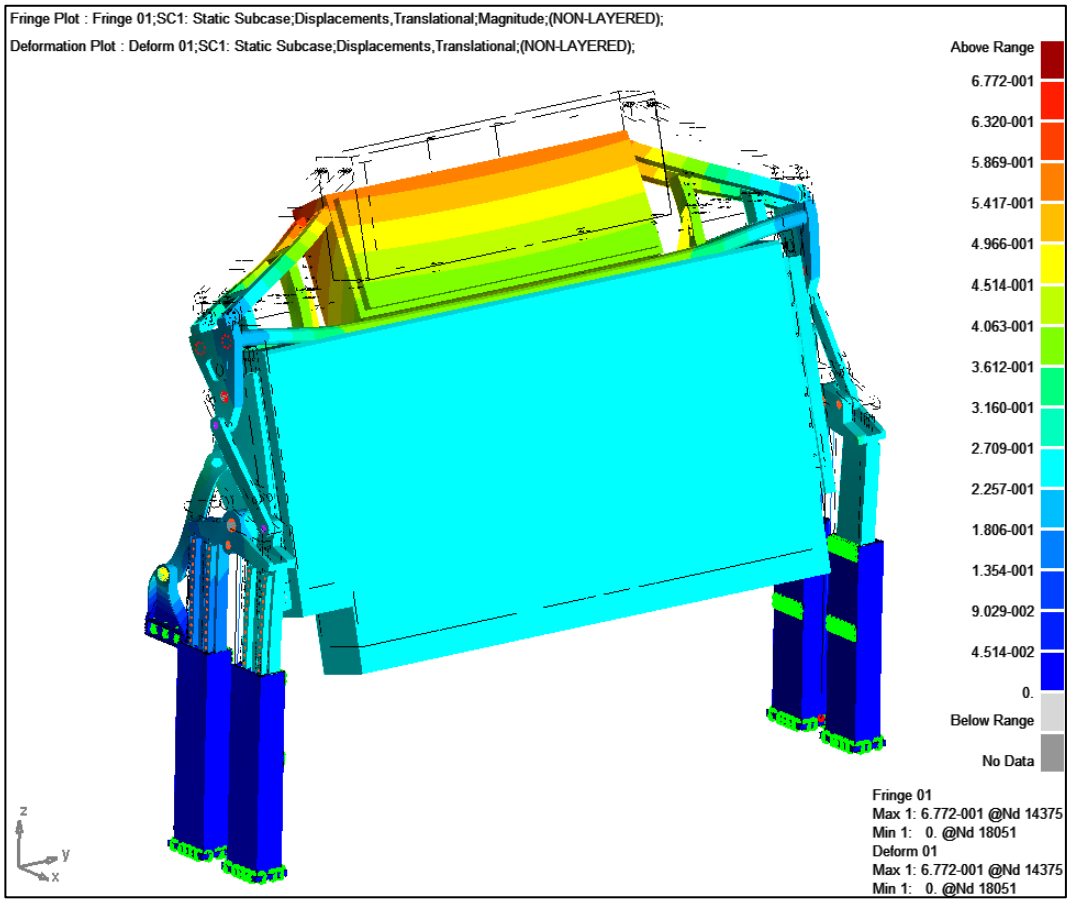

Figure 4.11. The Displacement of the System with Exaggerated Deformation

4.3.2. Flexible Multibody Dynamic Analysis

By using the existing finite element model, modal neutral files are created for each part to model the flexibility of the parts. Then, the flexible MBD model of the system is generated by defining appropriate constraints between the flexible parts. The flexible MBD model is illustrated in Figure 4.12.

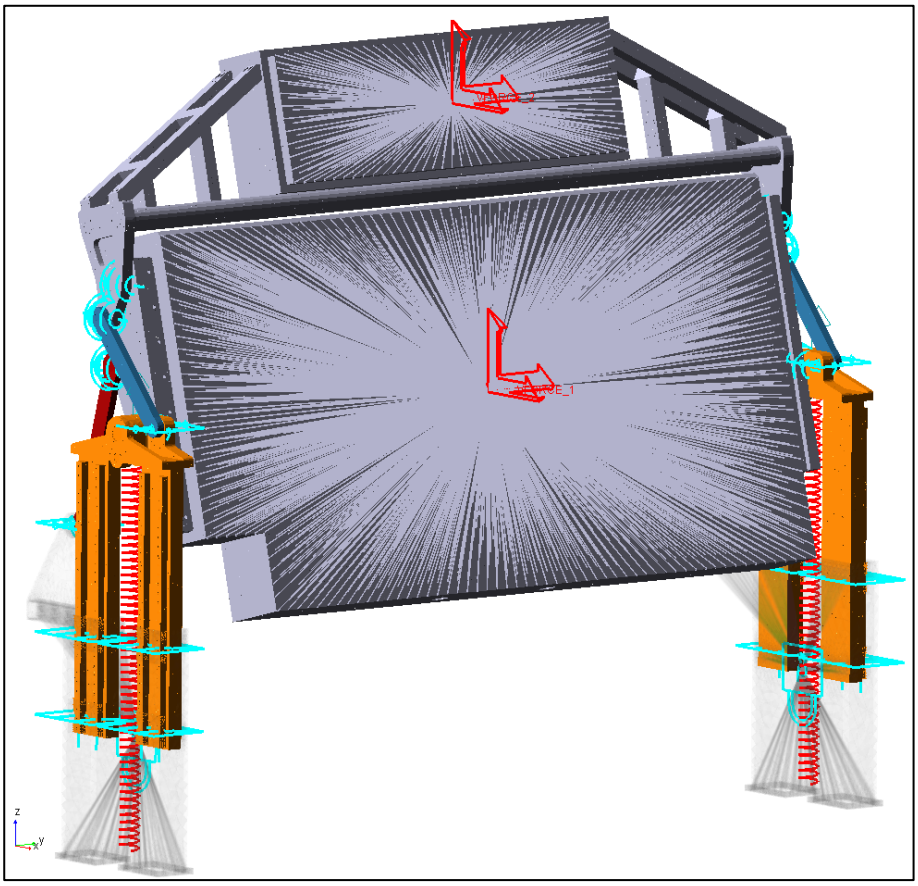

Figure 4.12. The Created Flexible MBD Model for the System

After the flexible MBD model is created, a dynamic analysis, which includes the inertial forces of the parts, is performed for the entire motion of the system. The simulation scenario is generated by considering the realistic working conditions of the system. Not only the gravitational forces, but also the exposed wind loads, which are obtained at the section 3.6.1, are modeled in the simulation scenario.

In simulation results, the maximum stress values on each part are examined in detail. As expected, the maximum stress on the system is observed in an intermediate position during the motion. As seen in Figure 4.13, the maximum value of the occurred stress is around 100 MPa which is acceptable for the material.

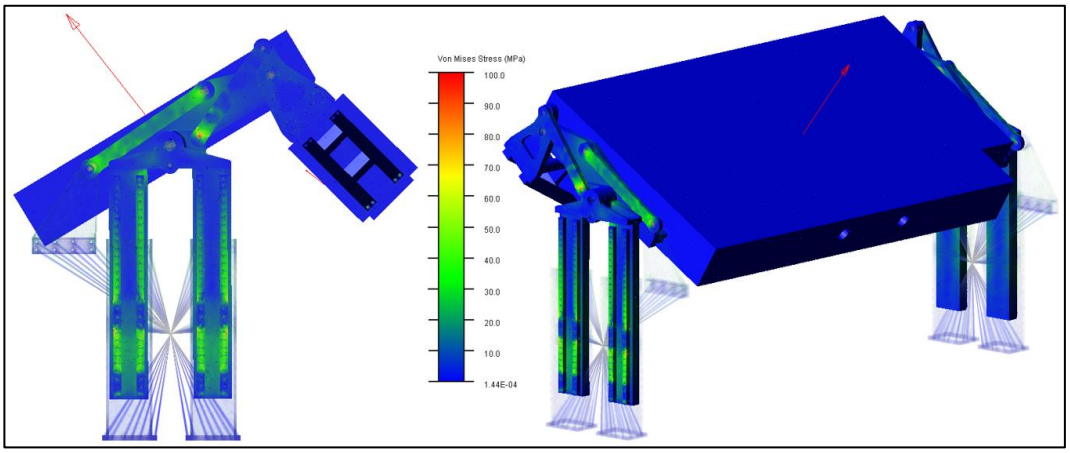

Figure 4.13. The Calculated Maximum Von Misses Stresses on the Folding Mechanism

CHAPTER 5

DISCUSSION AND CONCLUSION

In this study, the development of a folding mechanism for the two-antenna radar system is presented. Since the mechanism is developed for a military system, stringent repeatability and reliability requirements are considered in addition to the challenging geometric restrictions of the system. In order to provide the required rigidity and repeatability for the radar system, a folding mechanism with 1 DoF is aimed and realized unlike the similar products where the desired motion is achieved via multiple DoF mechanism. Therefore, a patent application to PCT (Patent Corporation Treaty) is filled for the developed mechanism concept, and the research step of the application is positively concluded.

During the study, a pre-prototype for the mechanism with a hydraulic actuator is manufactured with respect to the real physical properties to test the developed mechanism under different climatic conditions. Also, the pre-prototype is presented to the project team, and the expectations are discussed on the prototype. The manufactured pre-prototype is given in Figure 5.1.

Figure 5.1. The pre-prototype of the mechanism

Since the antennas are quite heavy, balancing the mechanism by replacing the center of gravities of antennas rather than placing an extra weight offers a significant improvement on the joint forces. In addition to the piston force requirement, the balancing study also reduces the exposed loads on the links. Further optimization studies on the dimensions of the mechanism can be performed as a future study.

Since the rigidity of the radar system at the operating position is crucial for the system performance, the links of the mechanism should be designed with respect to the results of the detailed strength and modal analyses. To give an example, as a result of the

modal analysis it is observed that there is a need for a locking mechanism between the links. After the modal analysis, the effect of the locking mechanisms on the system performance is also analyzed, and the use of the locking mechanism is evaluated simultaneously as seen in section 4.3.1. Additionally, the finite element model used for the analyses can be validated with the physical prototype by comparing the natural frequencies and the strains on the links.

REFERENCES

ASELSAN, Early Warning Radar System, www.aselsan.com.tr/en-us

ISKAR, 80K6M 3-D Air Surveillance Radar, Zaporizhzhia, www.iskra.zp.ua

Thales – Group, Ground Master – 400, www.thalesgroup.com/en/ground-master-400

Raytheon, AN/TPS-75, www.raytheon.com/capabilities/products/radar-systems

Condon, R. 2008. Motor Vehicle Having A Stowable Roof. U.S. Patent 0265610A1.

Queveau, G. 2002. Three-Part Folding Roof for Convertible Vehicles. U.S. Patent 6382703B1.

Pahl, G., Beitz, W. 1984. Engineering Design: A Systematic Approach, The Design Council, London, pp. 57-151

Erdman, A.G. 1984. Mechanism Design, Analysis and Synthesis Volume 1. Prentice – Hall.

Erdman, A.G. 1984. Mechanism Design, Analysis and Synthesis Volume 2. Prentice – Hall.

Freudenstein, F. 1954. An Analytical Approach to the Design of Four-Link Mechanisms. Transactions of the ASME, Vol. 76, 1954, pp.483-92.

Freudenstein, F., Primrose, E.J. 1972. The Classical Transmission-Angle Problem. The Institution of Mechanical Engineers. C96/72.

Soylemez, E. 2013. Mechanisms 4th Edition. Ankara.

Soylemez, E. 2015. Kinematic Synthesis Course Notes. Middle East Technical University. Ankara.

ADAMS User Guide, "Theory of Adams Flex", MSC Software, 2012

Sabatino M. 2007. Method and Apparatus for Propping Devices. U.S. Patent 0205338A1.